2.14. Fusion assay

NA cells in 48-well plates were transfected with 0.25 μg of the pCI vector encoding the G protein or pCI empty vector using TransIT-Neural according to the manufacturer's instructions. After 2 days post-transfection, cells were rinsed with each fusion medium, EMEM containing 10 mM 2-morpholinoethanesulfonic acid monohydrate (MES) and 10 mM N-2-hydroxyethyl-piperazine N′-2-ethanesulfonic acid (HEPES), adjusted to pH 5.8, 6.0 or 6.2 and replenished with the same fusion medium. After incubation at 37 °C for 30 min, cells were fixed with 4% paraformaldehyde and then stained with fuchsine solution. Images were obtained using *BIOREVO BZ-9000* (Keyence, Japan).

3. Results

3.1. Adaptation of street virus 1088 to NA cells after serial passaging

We performed the serial passage of 1088 in NA cells. In the first passage, the titer was only 2×10^5 FFU/ml although the cells were inoculated with 1088, hereafter 1088 (N0), at an MOI of 1. Meanwhile, at the 30th passage, the titer reached 10^8 FFU/ml. Then, the virus passaged 30 times, 1088-N30, was used for further analysis as an NA cell-adapted 1088 variant.

3.2. 1088-N30 had seven nucleotide substitutions

We compared the overall genomic sequences of 1088 (N0) and 1088-N30. Both genomes were 11,923 nucleotides (nt) in length, the same as several street viruses (Delmas et al., 2008; Faber et al., 2004; Ming et al., 2009; Szanto et al., 2008). Seven nucleotide substitutions were observed between the two viruses (Table 1). One nucleotide ambiguity was observed at nt 2513 of the 1088 (N0) genome, and three ambiguities were detected at nt 17, 28, and 1187 of the 1088-N30 genome. Three substitutions were detected in the non-coding region but not located in any known functional regions, such as start and stop signals for viral mRNA transcription. Three of four substitutions in the coding regions led to amino acid changes; two changes were located in the G protein. Of these, the change at position 196 from arginine to serine (R196S) led to the additional sequon at Asn^{194} (from Asn^{194}-Ser^{195}-Arg^{196} to Asn^{194}-Ser^{195}-Ser^{196}). *N*-Glycosylation typically occurs at the sequon Asn-X-Ser/Thr, where X is any amino acid except Pro. In addition, the amino acid at 333 of the G protein, one of the determinants of the virulence of the fixed viruses (Dietzschold et al., 1983; Seif et al., 1985; Takayama-Ito et al., 2006a; Tuffereau et al., 1989), did not change during the serial passage and was a virulent type Arg in both viruses.

3.3. Emergence of the R196S mutation corresponds to the increasing viral titer during serial passage

To determine when the mutations occurred, we examined nucleotide sequences during the series of passages. As shown in Fig. 1, the R196S mutation (A to T) emerged in the fourth passage, interestingly corresponding to the increase in the viral titer in NA cells. The T nucleotide became dominant in the sixth passage, whereas the A nucleotide was not detected in the ninth passage. Conversely, the P144L mutation in the G protein emerged in the seventh passage. At the site detected as ambiguous in the M gene (nt 2513), the A nucleotide was dominant in the 1088 (N0) genome (Table 1), but the G nucleotide became dominant in the seventh passage (data not shown). In addition, the mutation did not lead to an amino acid change. The other mutations occurred after the 14th passage (data not shown). Therefore, out of the mutations detected in the 1088-N30 genome, R196S was the first amino acid change and likely responsible for the adaptation to NA cells.

3.4. Cloning of the 1088 R196S variant

To obtain a 1088 variant that possesses only the R196S mutation in the G protein, we attempted cloning by limiting dilution from the virus stock of the fourth passage as described in Materials and methods. We picked out a clone designated 1088-N4#14 for further analysis. We determined the whole genome sequence of 1088-N4#14 and compared it with that of the 1088 (N0). In addition to R196S, the 1088-N4#14 genome had a mutation which leads to an amino acid substitution at position 61 from glycine to glutamate (G61E) in the P protein (Table 1). As the G61E mutation was also observed in several field isolates from terrestrial animals in the Americas (GenBank ID: AF369289, AF369308, AF369313, AF369323, AF369337, and AY998275), it probably does not affect the pathogenicity of street viruses.

3.5. In vitro characterization of 1088 and the 1088 variants

We examined the in vitro biological properties of 1088 (N0) and the 1088 variants. Initially, we checked the *N*-glycosylation status of the G protein (Fig. 2A). In the absence of the *N*-glycosylation inhibitor tunicamycin, both variant G proteins had less mobility than the 1088 (N0) G protein. In the presence of tunicamycin, the 1088-N30 G protein showed almost the same mobility as the 1088 (N0) G protein. A similar result was obtained when the G protein was expressed by a plasmid vector (Fig. 2B). Therefore, the R196S mutation solely leads to the additional *N*-glycosylation of the G protein.

Next, the growth kinetics of 1088 (N0) and the 1088 variants in NA cells were determined (Fig. 3A). At an MOI of 0.01, the 1088 variants replicated significantly better than 1088 (N0); their titers were four orders of magnitude higher than that of 1088 at 4 days p.i. Even at an MOI of 1, the 1088 variants replicated significantly better than 1088 (N0); the titers of 1088-N4#14 and 1088-N30 were three and two orders of magnitude higher than that of 1088 (N0) at 4 days p.i., respectively. These results indicate that 1088-N4#14 also adapted to NA cells as well as 1088-N30.

In addition, we determined the expression levels of the viral proteins in the MOI of 1 inoculation (Fig. 3B). Expression levels of the N protein increased in a time-dependent manner. Surprisingly, the levels were similar between the three viruses although the titers of 1088 (N0) were significantly lower than those of the variants (Fig. 3A). The G protein expression also increased in a time-dependent manner, however, the G protein was detected at low levels in the 1088-N30 infection compared with the 1088 (N0) and 1088-N4#14 infections throughout the indicated time points. Northern blot analysis revealed the mRNA expression of the G gene of 1088-30 to be at least as high as that of 1088 (N0) and 1088-N4#14 (Supplementary Fig. 1), indicating that the lower levels of the G protein of 1088-N30 were due to post-transcriptional events in the infected NA cells. In conclusion, the difference in the production of progeny viruses did not depend on the expression levels of viral proteins within the infected cells.

3.6. Both 1088 variants were attenuated in adult mice after intramuscular, but not intracerebral, inoculations

The pathogenicity of the three viruses was assessed in adult mice. After i.c. inoculations, both variants killed the adult mice as effectively as 1088 (N0), and the LD_{50} values of 1088 (N0), 1088-N4#14, and 1088-N30 were nearly identical (6.8, 6.8, and 5.0 FFU, respectively). Thus, 1088-N4#14 and 1088-N30 were not attenuated in neurovirulence in adult mice.

Table 1
Sequence differences between 1088 (N0), 1088-N4#14, and 1088-N30.

Nucleotide position	Region	Amino acid position	Nucleotide (amino acid)		
			1088 (N0)	1088-N4#14	1088-N30
17	Leader		T	T	T/C[a]
28	Leader		G	G	G/A[a]
1187	N gene	373	G (Glu)	G (Glu)	G/A[a] (Glu/Lys)
1695	P gene	61	G (Gly)	A (Glu)	G (Gly)
2513	M gene	6	A/G[b] (Lys)	A(Lys)	G (Lys)
3803	G gene	144	C (Pro)	C (Pro)	T (Leu)
3960	G gene	196	A (Arg)	T (Ser)	T (Ser)
11870	Trailer		A	A	G

[a] Signal strength was almost identical.
[b] The signal for the A nucleotide was dominant.

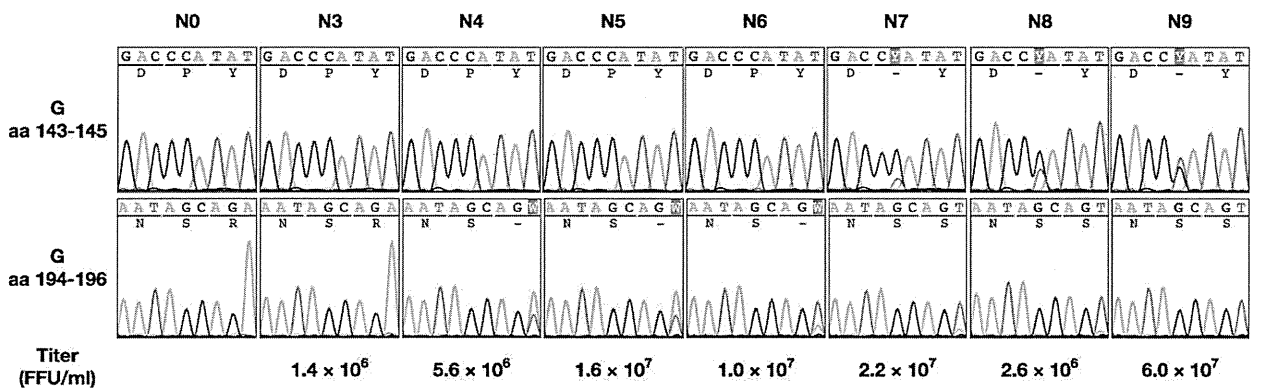

Fig. 1. Mutational events in the G gene during serial passaging. Sequence electropherograms of the G gene (amino acid regions from residues 143 to 145 and from residues 194 to 196) were obtained by RT-PCR and direct sequencing of virus stocks at the indicated passages. A titer in the supernatant for each passage is shown of the bottom.

Subsequently, we inoculated adult mice with serial dilutions (10^3–10^6 FFU) of each virus via the i.m. route (Table 2). At 10^6 FFU, all mice died from the 1088 (N0) infection, but all mice survived the 1088-N30 infection. Meanwhile, half of the mice survived the 1088-N4#14 infection. In total, 75% of mice inoculated with 1088 (N0) died, compared to only 10% of mice inoculated with 1088-N30. In the 1088-N4#14 infection, 30% of mice died in total, and a value intermediate between those for the 1088 (N0) and 1088-N30 infections. Therefore, 1088-N4#14 and 1088-N30 had reduced pathogenicity after the i.m. inoculation in adult mice although 1088-N4#14 showed moderate attenuation.

3.7. Distribution of viral antigens and humoral immune response in mice inoculated via the i.m. route

In order to investigate the events within the mice inoculated i.m., we prepared adult mice inoculated with each virus at 10^6 FFU and then collected serum, tissue and organ samples from five mice

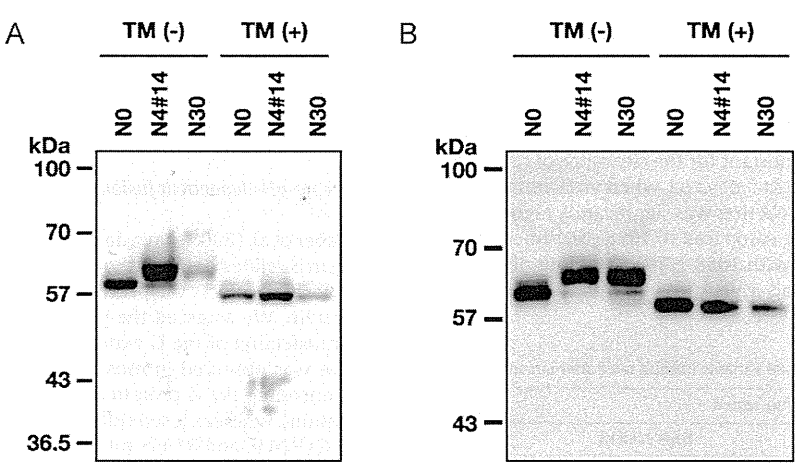

Fig. 2. *N*-Glycosylation of the G protein. Each virus was inoculated at an MOI of 1 (A), or each plasmid encoding the G protein was transfected into NA cells (B). The inoculated or transfected cells were incubated in the absence (–) or presence (+) of tunicamycin (TM, 1 μg/ml). The G proteins in the cells were detected by Western blotting using the anti-G antibody.

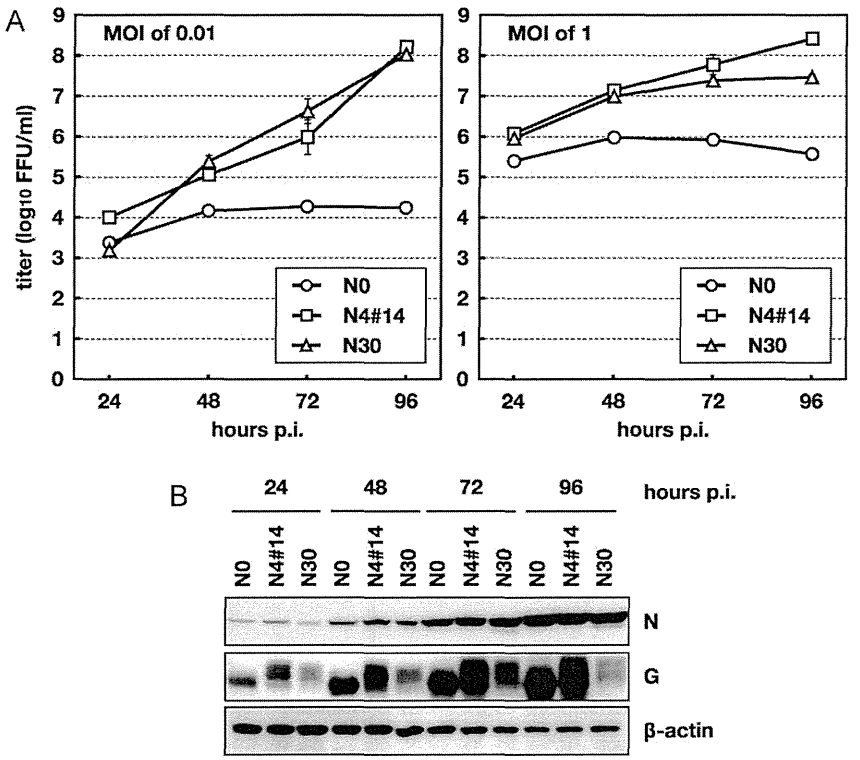

Fig. 3. (A) Virus growth curves in NA cells. Each virus was inoculated at an MOI of 0.01 or 1, and samples were collected at 24, 48, 72, and 96 h p.i. Titers represent the mean and standard deviation (SD) for three wells. (B) Viral proteins expressed in the infected NA cells at an MOI of 1. Lysates of the infected cells were prepared at the indicated time points, and viral proteins (N and G proteins) and β-actin were detected by Western blotting. 1088, (N0); 1088-N4#14, (N4#14); 1088-N30, (N30).

each at 5, 8, and 11 days p.i. after euthanasia. The viral spread within the CNS was examined by immunohistochemistry (Fig. 4A). At 5 days p.i., viral antigen-positive cells were detected in brain cortices, indicating that both 1088 variants were still neuroinvasive. At 8 and 11 days p.i., the viral antigen was widely distributed throughout the brain in the 1088 (N0)-infected mice. In contrast, its distribution was highly restricted in the 1088-N30-inoculated mice. Conversely, the distribution patterns for the 1088-N4#14 infection were intermediate between those for the 1088 (N0) and 1088-N30 infections. In other mice inoculated with 1088-N4#14, the patterns were varied, with some similar to the 1088 (N0) infections and some similar to the 1088-N30 infections (Supplementary Fig. 2). The results for the 1088-N4#14 infection seem to represent a rate of lethality of 50%.

We also checked the VNA titer in serum of the infected mice because the response is important for the clearance of rabies virus (Hooper et al., 1998, 2009). At 5 days p.i. when viral antigens were detected in the cortex, the VNA titer was significantly higher in mice infected with 1088 variants compared to 1088 (N0)-infected mice (Fig. 4B). All mice infected with 1088-N4#14 and four of five mice infected with 1088-N30 had a VNA titer of more than 0.5 IU/ml, the criterion for preventing rabies (World Health Organ, 2005), whereas only one of five mice infected with 1088 (N0) had a VNA titer of more than 0.5 IU/ml. The tendency for the variants to induce a greater response than 1088 (N0) was also observed at 8 and 11 days p.i., although all of the mice infected with 1088 (N0) had a VNA titer above 0.5 IU/ml.

Table 2
Pathogenicity of 1088 (N0) and 1088 variants in adult mice after i.m. inoculations.

Dose (FFU)	No. dead/no. tested		
	1088 (N0)	1088-N4#14	1088-N30
10^6	10/10	5/10	0/10
10^5	7/10	5/10	1/10
10^4	8/10	0/10	3/10
10^3	5/10	2/10	1/10
Total	30/40	12/40	4/40

3.8. Kinetics of virus entry into NA cells

In the case of SHBRV-18, efficient internalization into NA cells is responsible for the neruroinvasiveness (Faber et al., 2004). As shown above, however, the 1088 variants were still neuroinvasive. Not surprisingly, no obvious differences were observed in internalization efficiency between the three viruses (Fig. 5).

3.9. Low-pH-dependent fusion of the G protein in transfected cells

Faber et al. (2005) have demonstrated that position 194 of the G protein is related to the pathogenicity of the virus and a mutation at this position affects the pH threshold for membrane fusion by the G protein. We assessed the pH-dependent cell fusion in NA cells by transfection of the G expression vector (Fig. 6). At pH 6.0, cell fusion was observed in most NA cells transfected with the plasmid encoding the G protein of 1088 (N0) or 1088-N4#14 (R196S mutation), whereas fused cells were rarely recognized in the 1088-N30 G (P144L and R196S mutations) transfection. Cell fusion was observed clearly in the cells transfected with the G protein of 1088-N30 at pH 5.8, but rarely recognized in any G transfection at pH 6.2. Hence, the pH threshold of the G protein of 1088-N30 was lower than that of pH compared to the G protein of 1088 (N0) or 1088-N4#14.

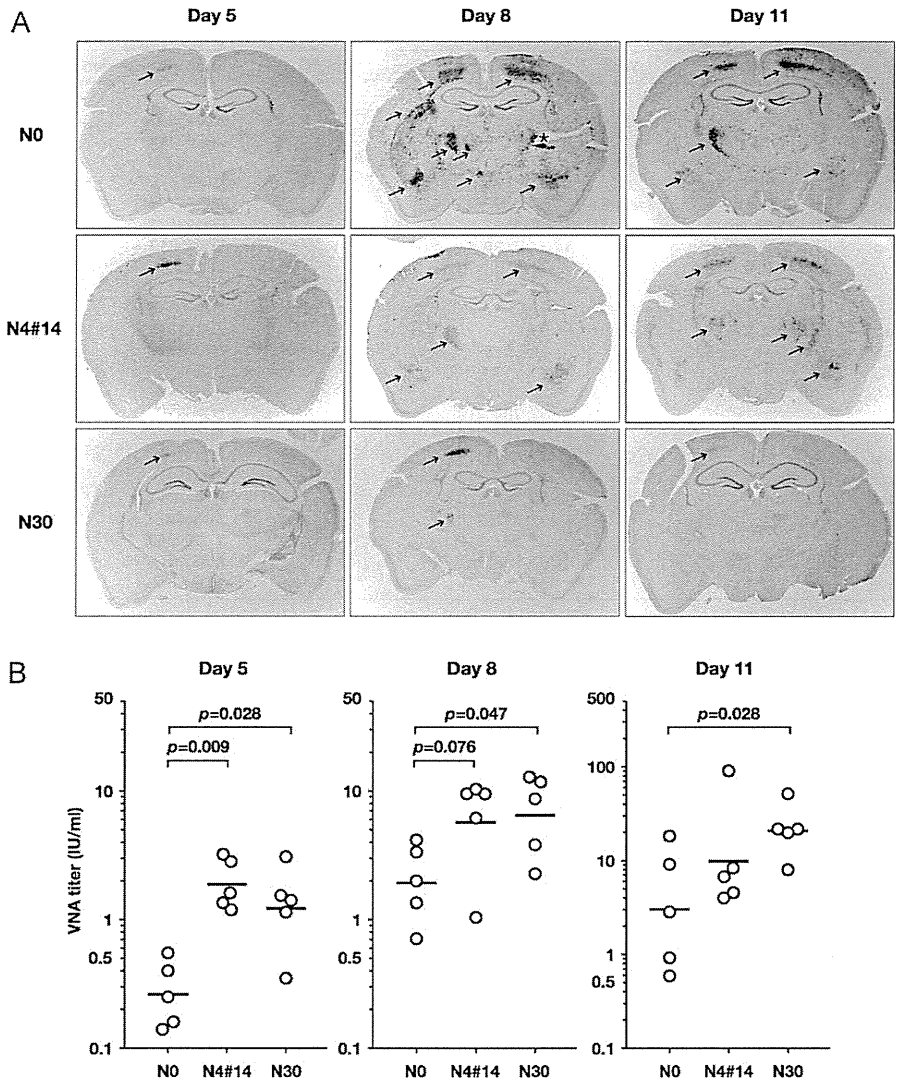

Fig. 4. Mice (15 per group) were inoculated with 1088 (N0), 1088-N4#14 (N4#14), or 1088-N30 (N30) via the i.m. route at 10^6 FFU. At 5, 8 and 11 days p.i., 5 mice per group were sacrificed and their sera, tissues, and organs were sampled. (A) Immunohistochemical analysis of viral antigens in the inoculated mouse brain at different time points. Coronal sections of the mouse brain were stained with anti-P serum. Each image is representative of five individual mice at each time point. Arrows indicate P-protein-positive cells. The asterisk indicates an artifact. (B) VNA responses in the mice. VNA titers were determined by RFFIT and represented as IU/ml. Each open circle in the graphs shows a VNA titer in individual mouse serum. All mock-injected mice showed <0.2 IU/ml (data not shown). Bars represent geometric means. *P* values in the graphs were determined by Mann–Whitney's *U* test. Only *P* values less than 0.1 were indicated.

4. Discussion

Parasites, including viruses, are generally attenuated in an original host during serial passage in a new host (e.g., cell cultures), in part because of a loss of pathogenicity due to the accumulation of deleterious mutations (Ebert, 1998). Current fixed rabies virus strains have been established by serial passage of street viruses in animal brains, tissues and/or cell lines. Most fixed viruses show a reduction or loss of pathogenesis on inoculation via peripheral sites although they are still neurovirulent. Pathogenicity on infection via peripheral sites is one of the phenotypes characterizing street viruses. Since pathogenicity is important to the transmission and circulation of rabies viruses in nature but not under laboratory conditions, the fixed viruses have lost the ability presumably because mutations have emerged and become fixed during serial passaging due to the absence of negative selection. Interestingly, it was demonstrated that attenuated fixed viruses reverted to neurovirulent after a few passages in neuroblastoma cell lines (Clark, 1978). Therefore, we speculated that neurovirulence is maintained during serial passaging in neuroblastoma cells but the phenotype(s) specific to street viruses is not. Hence, we performed the serial passage of street virus 1088 in mouse neuroblastoma NA cells and succeeded in establishing a variant, 1088-N30, which was attenuated in mice after i.m. but not i.c. inoculations.

Most fixed viruses have three or four potential glycosylation sites on the G protein, and two sequons at Asn^{37} and Asn^{319} are common in fixed viruses (Morimoto et al., 1992). The sequon at Asn^{319} is conserved in all known lyssaviruses (Badrane and Tordo, 2001), and the sequon at Asn^{37} is not efficiently glycosylated (Shakin-Eshleman et al., 1992). Ming et al. (2009) mentioned that several street viruses lack the sequon at Asn^{247} observed in several fixed viruses. Indeed, street viruses whose entire genome has been sequenced possess one or two potential *N*-glycosylation sites in the G protein (as summarized in Table 3). Moreover, most of

Table 3
Potential *N*-glycosylation sites on the G protein of street and fixed rabies viruses.

Strain	Origin	Location	Year	*N*-Glycosylation sites (potential[a])	GenBank accession no.	Ref.
Street viruses						
1088	Woodchuck	USA	1970s	37, 319	AB645847	This work
BR-Pfx1	Fox	Brazil	2002	37, 319	AB362483	Mochizuki et al. (2009)
HN10	Human	China	2006	37, 319	EU643590	Ming et al. (2009)
NNV-RAB-H	Human	India		37, 319	EF437215	Nagaraja et al. (2008)
H-08-1320	Human	Sri Lanka	2008	37, 319	AB569299	Matsumoto et al. (2011)
8743THA[b]	Human	Thailand	1983	37, 319	EU293121	Delmas et al. (2008)
8764THA	Human	Thailand	1983	37, 319	EU293111	Delmas et al. (2008)
9001FRA	Dog[c]	French Guyana	1991	37, 319	EU293115	Delmas et al. (2008)
9147FRA	Fox	France	1990	37, 319	EU293113	Delmas et al. (2008)
9704ARG	Bat	Argentina	1997	319	EU293116	Delmas et al. (2008)
RRV ON-99-2	Raccoon	USA	1999	319	EU311738	Szanto et al. (2008)
SHBRV-18	Bat	USA		237, 319	AY705373	Faber et al. (2004)
Fixed viruses						
CVS-11				37, 204, 319	EU352767	Wright et al. (2008)
Pitman Moore	Vaccine			37, 204, 319	AJ871962	
ERA	Vaccine			37, 247, 319	EF206707	Geue et al. (2008)
SAD B19	Vaccine			37, 247, 319	M31046	Conzelmann et al. (1990)
RV-97	Vaccine			37, 247, 319	EF542830	Metlin et al. (2008)
Nishigahara	Vaccine			37, 247, 319	AB044824	Ito et al. (2001a)
RC-HL	Vaccine			37, 247, 319	AB009663	Ito et al. (2001a)
PV	Vaccine			37, 158, 247, 319	M13215	Tordo et al. (1986)
HEP-Flury	Vaccine			37, 158, 319	M32751	Morimoto et al. (1989)

[a] Sequons in ectodomain.
[b] Passaged 22 times in BSR cells.
[c] Bitten by a bat.

the G sequences of field isolates available in GenBank also possess only one or two potential *N*-glycosylation sites (Asn^{319}, or Asn^{37} and Asn^{319}), although the SHBRV-18 G protein has sequons at Asn^{237} and Asn^{319}. Thus, it is likely that the *N*-glycosylation of the G protein is strictly subjected to the pressures of natural selection because there is some disadvantage for street viruses. In the present study, we found that the G protein of 1088 (N0) possesses only two potential *N*-glycosylation sites, at Asn^{37} and Asn^{319}, whereas 1088-N30 has three sites as well as fixed strains. In order to demonstrate that the additional *N*-glycosylation affects the phenotype(s) of the street virus, we attempted to select a cloned variant that has the *N*-glycosylation mutation only. Although, unfortunately, we could not obtain such a variant, we selected 1088-N4#14, which has another mutation in addition to the *N*-glycosylation mutation. We found that 1088-N4#14 and 1088-N30 were less pathogenic in adult mice than the parental 1088 after i.m. inoculations, although 1088-N4#14 was not highly attenuated. The reduced pathogenicity in the i.m. infection, even if not highly attenuated, would affect viral transmission and circulation. The mutation in the P protein of 1088N4#14 (Glu at position 61) is also found in several street virus strains, indicating that it is not likely to impair the pathogenesis. Therefore, the additional *N*-glycosylation is likely involved in the reduced pathogenicity though it is not the sole determinant of the attenuated phenotype of 1088-N30. Consequently, we think that under natural conditions, the street virus population in which the mutation leading to additional *N*-glycosylation has arisen may be negatively selected.

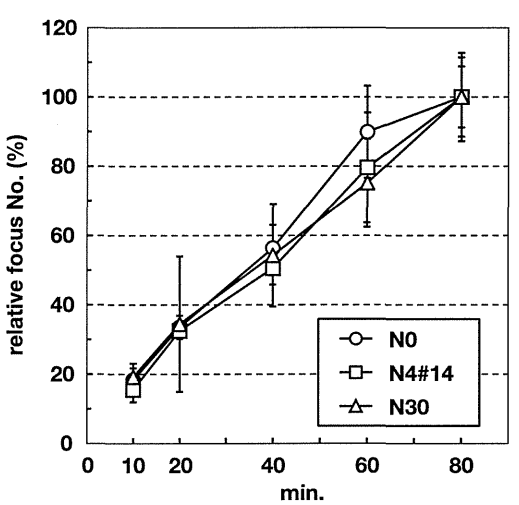

Fig. 5. Efficiency of virus internalization in NA cells. The same titer of virus was added to each well and then incubated for the period indicated at 37 °C. After incubation, the cells were washed and overlaid with medium containing methylcellulose. Viral foci derived from internalized viruses were visualized at 4 days p.i. and the internalization efficiency of each strain is indicated as the relative number of foci, taking the number at 80 min as 100%. Values represent the mean ± SD from four individual wells.

We found a correlation between the attenuation of 1088-N30 and induction of a humoral immune response. It is likely that the induction of a strong immune response is one of the factors responsible for the attenuation of 1088-N30. The highly restricted spread of 1088-N30 in the CNS after the i.m. inoculation is probably due to a strong immune response rather than a loss of ability for neuron-to-neuron spread, because 1088-N30 was still pathogenic after the i.c. inoculation. Indeed, the street virus strain SHBRV induced weak innate immune responses compared with an attenuated fixed virus (Wang et al., 2005). Several lines of evidence indicate that immune evasion of street viruses is important for pathogenicity through the maintenance of the BBB's integrity to prevent immune effectors entering the CNS (Kuang et al., 2009; Roy and Hooper, 2007, 2008; Roy et al., 2007). From our results, although the possibility that the G protein with the additional *N*-glycosylation had enhanced immunogenicity itself could not be ruled out, the marked enhancement of virus production is a rational explanation for the induction of the strong immune response.

Interestingly, Faber et al. (2005) reported that the Asn residue at position 194 of the G protein is related to pathogenicity. On comparing two Asn^{194} mutants, one virulent and one avirulent, they found that the virulent mutant showed enhanced internalization

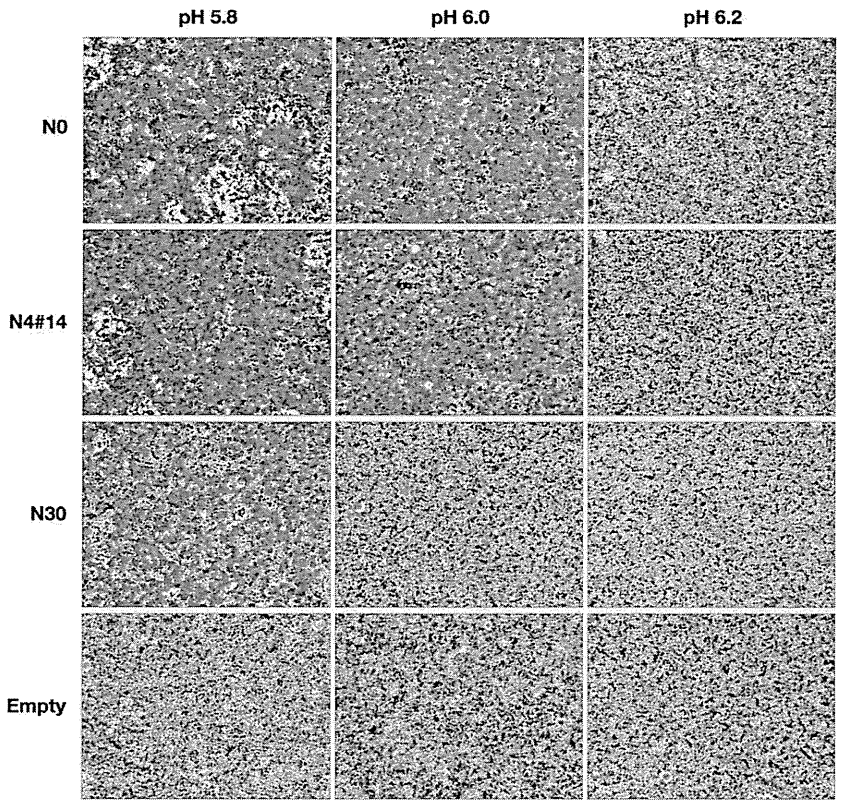

Fig. 6. Low-pH cell fusion by the G protein. NA cells were transfected with a plasmid encoding the G protein of 1088 (N0), 1088-N4#14 (N4#14), or 1088-N30 (N30). Empty vector was also transfected. At 2 days after the transfection, the cells were treated with fusion medium at the indicated pH and incubated at 37 °C for 30 min. Fused cells were stained with fuchsine solution.

efficiency in cells, enhanced cell-to-cell spread, and a higher pH threshold of membrane fusion activity by the G protein. Therefore, the *N*-glycosylation at Asn^{194} was likely to affect these characteristics. However, we did not detect a difference in internalization efficiency and pH threshold between the parental 1088 and 1088-N4#14 (Figs. 5 and 6). Furthermore, contrary to their result, the 1088 variants made larger foci than the parental strain in NA cells (our unpublished observation). Hence, the mechanism of attenuation via *N*-glycosylation at Asn^{194} is different from that via the mutation at position 194 without *N*-glycosylation reported previously.

Although 1088-N4#14 induced a humoral immune response as strongly as did 1088-N30, it exhibited intermediate pathogenicity between that of 1088 (N0) and 1088-N30. The other mutations are also probably related to the greater attenuation. Prehaud et al. (1988) demonstrated that one escape mutant of the CVS strain selected with a MAb against antigenic site II of the G protein was 300 times less pathogenic than the parental CVS after i.m. inoculation. The mutant had an amino acid mutation at position 147. The region around position 147 including position 144 is also likely important to the pathogenicity. Indeed, we found that the 1088-N30 G protein (P144L and R196S mutations), but not the 1088-N4#14 G protein (R196S mutation), had a lower pH threshold of membrane fusion activity than the G protein of 1088. As described above, Faber et al. (2005) demonstrated a correlation between a lower pH threshold and attenuation. Therefore, the P144L mutation might be more closely related to the attenuated phenotype of 1088-N30 than the R196S mutation. In addition, since the Pro at position 144 is absolutely conserved among the G proteins deposited in GenBank (our unpublished observation), position 144 is probably important to the pathogenicity of the street viruses.

Mutations in the leader and trailer sequences (nt 17, 28, and 11870), and N protein (E373E/K) of 1088-N30 also have the potential to be involved in the greater attenuation. Indeed, Faber et al. (2004) reported that the trailer sequence could modulate the pathogenicity of SHBRV, and the involvement of leader and trailer sequences in the viral pathogenesis has also reported in other *Mononegavirales* (Banyard et al., 2005; Fujii et al., 2002). On the other hand, Masatani et al. (2010) demonstrated that the N protein of a pathogenic fixed strain functioned to evade retinoic acid-inducible gene I (RIG-I)-mediated antiviral responses but that of an attenuated strain did not. Therefore, the attenuated strain strongly activated expression of interferon and chemokine genes in infected cells. They also reported that amino acids at positions 273 and 394 of the N protein are important for the evasion and pathogenesis (Masatani et al., 2011). Intriguingly, the latter is located near the mutation detected in the N gene of 1088-N30.

We cannot rule out the possibility that the mutation detected in the P protein of 1088-N4#14 disguises the attenuating effects of the R196S mutation. The Glu residue at position 61 of the P protein was also detected in several field isolates from terrestrial animals, the sequences of which are available in GenBank. Therefore, it is possible that the mutation enhances rather than impairs the pathogenicity as mentioned above. It has been demonstrated that the P protein functions to interfere with the interferon system (Brzozka et al., 2005, 2006; Ito et al., 2010; Rieder et al., 2011; Vidy et al., 2005) and interact with dynein light chain LC8 (Jacob et al., 2000; Raux et al., 2000). The interaction is slightly related to

the pathogenicity (Mebatsion, 2001; Rasalingam et al., 2005). However, position 61 is outside of the domains identified as important for functions.

Both 1088 variants showed much better proliferative activity than the parental 1088 in NA cells. Therefore, the additional *N*-glycosylation, common mutation to both variants, is likely responsible for the adaptation. It seems that the additional *N*-glycosylation enhanced the release of viral particles from the cells, since the expression levels of viral proteins were similar between 1088 (N0) and 1088-N4#14 at an MOI of 1 (Fig. 3B). Interestingly, in the case of WNV, the *N*-glycosylated E protein enhanced the viral replication efficiency in cell lines (Beasley et al., 2005; Li et al., 2006; Shirato et al., 2004), and WNV whose E protein was glycosylated budded from the cell surface but the non-glycosylated variant budded at intracellular membranes (Li et al., 2006). This is also likely in the present case. Several ultrastructural studies have demonstrated that street viruses matured by budding at intracellular membranes, such as the endoplasmic reticulum (ER), but fixed viruses preferred to bud from the plasma membrane in cultured neural cells and within the CNS (Fekadu et al., 1982; Iwasaki et al., 1975; Iwasaki and Tobita, 2002; Matsumoto et al., 1974; Matsumoto and Yonezawa, 1971; Murphy et al., 1973). The mechanism by which the additional *N*-glycosylation of the G protein enhances viral production should be elucidated by further investigation.

While 1088-N30 showed strong growth in NA cells, its G protein was expressed at a lower level than that of 1088 (N0) or 1088-N4#14 (Fig. 3B). A similar result was found in Fig. 2A. This was not due to the sensitivity of the anti-G MAb 15-13, because the 1088-N30 G protein was detected at the same level as the 1088 (N0) and 1088-N4#14 G proteins by this MAb when the G proteins were expressed using a plasmid vector (Fig. 2B). Moreover, the MAb 15-13 recognizes a linear epitope containing the amino acid at position 251 of the G protein (Luo et al., 1997). Furthermore, the G mRNA levels of 1088-30 were similar to those of 1088 (N0) and 1088-N4#14 (Supplementary Fig. 1). Therefore, the low expression of the G protein of 1088-N30 was due to post-transcriptional events in the infected cells. Generally, newly synthesized glycoproteins undergo proper folding by chaperons in the ER, whereas misfolded proteins are eliminated via the ER-associated degradation (ERAD) pathway, in which misfolded proteins are retrotranslocated from the ER to the cytoplasm and then degraded by the proteasome (Ruddock and Molinari, 2006). It was reported that the hepatitis C virus activates the ERAD pathway and that the half-life of viral glycoproteins in infected cells increased when ERAD was inhibited (Saeed et al., 2011). Thus, the ERAD pathway might be activated in the 1088-N30-infected cells but not 1088 (N0)- or 1088-N4#14-infected cells, or the 1088-N30 G protein might be more easily degraded under conditions in which ERAD is facilitated. In addition, the reason why 1088-N30 multiplied efficiently in NA cells in spite of low levels of the G protein might be that the G protein's expression is not a rate-determining factor for viral production in 1088-N30-infected NA cells.

In this study, by comparing strains with different virulence but with very similar genomic sequences, we could discuss the viral elements related to the pathogenicity of street viruses at the nucleotide and amino acid levels. Then, we found a relationship between the *N*-glycosylation of the rabies virus G protein and biological activities such as growth ability and pathogenicity. Database analysis suggests that the number of *N*-glycosylation sites in the G protein is limited in field isolates, and is probably under natural selection. In support of this, our results indicate that the additional *N*-glycosylation might interfere with the pathogenicity required for circulation in nature, although it is an adaptive mutation in NA cells. However, since the *N*-glycosylation at Asn^{194} is novel in the rabies virus and 1088-N4#14 has another mutation, it should be confirmed whether the additional *N*-glycosylation at Asn^{194} is solely responsible for the attenuation of 1088 and other street strains. Generalizing the concept presented here would be one way to facilitate understanding of the pathogenicity of rabies viruses. For this, further investigation is required to assess whether the additional *N*-glycosylation observed in fixed viruses (at Asn^{158}, Asn^{204}, or Asn^{247}) also affects the pathogenicity of street viruses.

Acknowledgements

We thank Dr. M. Sugiyama (Gifu University, Gifu, Japan) for providing the anti-G MAb 15-13.

This study was supported in part by grants from the Ministry of Education, Culture, Sports, Science and Technology of Japan (no. 21780278) and from the Ministry of Health, Labour and Welfare of Japan.

Appendix A. Supplementary data

Supplementary data associated with this article can be found, in the online version, at doi:10.1016/j.virusres.2012.01.002.

References

Badrane, H., Tordo, N., 2001. Host switching in Lyssavirus history from the Chiroptera to the Carnivora orders. J. Virol. 75, 8096–8104.
Baer, M.G., 2007. The history of rabies. In: Jackson, A.C., Wunner, W.H. (Eds.), Rabies. , 2nd ed. Academic Press, San Diego, pp. 1–22.
Banyard, A.C., Baron, M.D., Barrett, T., 2005. A role for virus promoters in determining the pathogenesis of Rinderpest virus in cattle. J. Gen. Virol. 86, 1083–1092.
Beasley, D.W., Whiteman, M.C., Zhang, S., Huang, C.Y., Schneider, B.S., Smith, D.R., Gromowski, G.D., Higgs, S., Kinney, R.M., Barrett, A.D., 2005. Envelope protein glycosylation status influences mouse neuroinvasion phenotype of genetic lineage 1 West Nile virus strains. J. Virol. 79, 8339–8347.
Brzozka, K., Finke, S., Conzelmann, K.K., 2005. Identification of the rabies virus alpha/beta interferon antagonist: phosphoprotein P interferes with phosphorylation of interferon regulatory factor 3. J. Virol. 79, 7673–7681.
Brzozka, K., Finke, S., Conzelmann, K.K., 2006. Inhibition of interferon signaling by rabies virus phosphoprotein P: activation-dependent binding of STAT1 and STAT2. J. Virol. 80, 2675–2683.
Clark, H.F., 1978. Rabies viruses increase in virulence when propagated in neuroblastoma cell culture. Science 199, 1072–1075.
Conzelmann, K.K., Cox, J.H., Schneider, L.G., Thiel, H.J., 1990. Molecular cloning and complete nucleotide sequence of the attenuated rabies virus SAD B19. Virology 175, 485–499.
Delmas, O., Holmes, E.C., Talbi, C., Larrous, F., Dacheux, L., Bouchier, C., Bourhy, H., 2008. Genomic diversity and evolution of the lyssaviruses. PLoS One 3, e2057.
Dietzschold, B., Morimoto, K., Hooper, D.C., Smith, J.S., Rupprecht, C.E., Koprowski, H., 2000. Genotypic and phenotypic diversity of rabies virus variants involved in human rabies: implications for postexposure prophylaxis. J. Hum. Virol. 3, 50–57.
Dietzschold, B., Wiktor, T.J., Trojanowski, J.Q., Macfarlan, R.I., Wunner, W.H., Torres-Anjel, M.J., Koprowski, H., 1985. Differences in cell-to-cell spread of pathogenic and apathogenic rabies virus in vivo and in vitro. J. Virol. 56, 12–18.
Dietzschold, B., Wunner, W.H., Wiktor, T.J., Lopes, A.D., Lafon, M., Smith, C.L., Koprowski, H., 1983. Characterization of an antigenic determinant of the glycoprotein that correlates with pathogenicity of rabies virus. Proc. Natl. Acad. Sci. U. S. A. 80, 70–74.
Ebert, D., 1998. Experimental evolution of parasites. Science 282, 1432–1435.
Etessami, R., Conzelmann, K.K., Fadai-Ghotbi, B., Natelson, B., Tsiang, H., Ceccaldi, P.E., 2000. Spread and pathogenic characteristics of a G-deficient rabies virus recombinant: an in vitro and in vivo study. J. Gen. Virol. 81, 2147–2153.
Faber, M., Faber, M.L., Papaneri, A., Bette, M., Weihe, E., Dietzschold, B., Schnell, M.J., 2005. A single amino acid change in rabies virus glycoprotein increases virus spread and enhances virus pathogenicity. J. Virol. 79, 14141–14148.
Faber, M., Pulmanausahakul, R., Nagao, K., Prosniak, M., Rice, A.B., Koprowski, H., Schnell, M.J., Dietzschold, B., 2004. Identification of viral genomic elements responsible for rabies virus neuroinvasiveness. Proc. Natl. Acad. Sci. U. S. A. 101, 16328–16332.
Fekadu, M., Chandler, F.W., Harrison, A.K., 1982. Pathogenesis of rabies in dogs inoculated with an Ethiopian rabies virus strain. Immunofluorescence, histologic and ultrastructural studies of the central nervous system. Arch. Virol. 71, 109–126.
Fujii, Y., Sakaguchi, T., Kiyotani, K., Huang, C., Fukuhara, N., Egi, Y., Yoshida, T., 2002. Involvement of the leader sequence in Sendai virus pathogenesis revealed by recovery of a pathogenic field isolate from cDNA. J. Virol. 76, 8540–8547.
Geue, L., Schares, S., Schnick, C., Kliemt, J., Beckert, A., Freuling, C., Conraths, F.J., Hoffmann, B., Zanoni, R., Marston, D., McElhinney, L., Johnson, N., Fooks, A.R., Tordo, N., Muller, T., 2008. Genetic characterisation of attenuated. SAD rabies virus strains used for oral vaccination of wildlife. Vaccine 26, 3227–3235.

Hooper, D.C., Morimoto, K., Bette, M., Weihe, E., Koprowski, H., Dietzschold, B., 1998. Collaboration of antibody and inflammation in clearance of rabies virus from the central nervous system. J. Virol. 72, 3711–3719.
Hooper, D.C., Phares, T.W., Fabis, M.J., Roy, A., 2009. The production of antibody by invading B cells is required for the clearance of rabies virus from the central nervous system. PLoS Negl. Trop. Dis. 3, e535.
Ito, N., Kakemizu, M., Ito, K.A., Yamamoto, A., Yoshida, Y., Sugiyama, M., Minamoto, N., 2001a. A comparison of complete genome sequences of the attenuated RC-HL strain of rabies virus used for production of animal vaccine in Japan, and the parental Nishigahara strain. Microbiol. Immunol. 45, 51–58.
Ito, N., Moseley, G.W., Blondel, D., Shimizu, K., Rowe, C.L., Ito, Y., Masatani, T., Nakagawa, K., Jans, D.A., Sugiyama, M., 2010. Role of interferon antagonist activity of rabies virus phosphoprotein in viral pathogenicity. J. Virol. 84, 6699–6710.
Ito, N., Takayama, M., Yamada, K., Sugiyama, M., Minamoto, N., 2001b. Rescue of rabies virus from cloned cDNA and identification of the pathogenicity-related gene: glycoprotein gene is associated with virulence for adult mice. J. Virol. 75, 9121–9128.
Iwasaki, Y., Ohtani, S., Clark, H.F., 1975. Maturation of rabies virus by budding from neuronal cell membrane in suckling mouse brain. J. Virol. 15, 1020–1023.
Iwasaki, Y., Tobita, M., 2002. Pathology. In: Jackson, A.C., Wunner, W.H. (Eds.), Rabies. Academic Press, San Diego, pp. 283–306.
Jacob, Y., Badrane, H., Ceccaldi, P.E., Tordo, N., 2000. Cytoplasmic dynein LC8 interacts with lyssavirus phosphoprotein. J. Virol. 74, 10217–10222.
Kojima, D., Park, C.H., Tsujikawa, S., Kohara, K., Hatai, H., Oyamada, T., Noguchi, A., Inoue, S., 2010. Lesions of the central nervous system induced by intracerebral inoculation of BALB/c mice with rabies virus (CVS-11). J. Vet. Med. Sci. 72, 1011–1016.
Kuang, Y., Lackay, S.N., Zhao, L., Fu, Z.F., 2009. Role of chemokines in the enhancement of BBB permeability and inflammatory infiltration after rabies virus infection. Virus Res. 144, 18–26.
Lepine, P., 1938. On the evolution of fixed strains of rabies virus. J. Hyg. (Lond.) 38, 180–184.
Li, J., Bhuvanakantham, R., Howe, J., Ng, M.L., 2006. The glycosylation site in the envelope protein of West Nile virus (Sarafend) plays an important role in replication and maturation processes. J. Gen. Virol. 87, 613–622.
Luo, T.R., Minamoto, N., Hishida, M., Yamamoto, K., Fujise, T., Hiraga, S., Ito, N., Sugiyama, M., Kinjo, T., 1998. Antigenic and functional analyses of glycoprotein of rabies virus using monoclonal antibodies. Microbiol. Immunol. 42, 187–193.
Luo, T.R., Minamoto, N., Ito, H., Goto, H., Hiraga, S., Ito, N., Sugiyama, M., Kinjo, T., 1997. A virus-neutralizing epitope on the glycoprotein of rabies virus that contains Trp251 is a linear epitope. Virus Res. 51, 35–41.
Masatani, T., Ito, N., Shimizu, K., Ito, Y., Nakagawa, K., Abe, M., Yamaoka, S., Sugiyama, M., 2011. Amino acids at positions 273 and 394 in rabies virus nucleoprotein are important for both evasion of host RIG-I-mediated antiviral response and pathogenicity. Virus Res. 155, 168–174.
Masatani, T., Ito, N., Shimizu, K., Ito, Y., Nakagawa, K., Sawaki, Y., Koyama, H., Sugiyama, M., 2010. Rabies virus nucleoprotein functions to evade activation of the RIG-I-mediated antiviral response. J. Virol. 84, 4002–4012.
Matsumoto, S., Schneider, L.G., Kawai, A., Yonezawa, T., 1974. Further studies on the replication of rabies and rabies-like viruses in organized cultures of mammalian neural tissues. J. Virol. 14, 981–996.
Matsumoto, S., Yonezawa, T., 1971. Replication of rabies virus in organized cultures of Mammalian neural tissues. Infect. Immun. 3, 606–616.
Matsumoto, T., Ahmed, K., Wimalaratne, O., Yamada, K., Nanayakkara, S., Perera, D., Karunanayake, D., Nishizono, A., 2011. Whole-genome analysis of a human rabies virus from Sri Lanka. Arch. Virol. 156, 659–669.
Mebatsion, T., 2001. Extensive attenuation of rabies virus by simultaneously modifying the dynein light chain binding site in the P protein and replacing Arg333 in the G protein. J. Virol. 75, 11496–11502.
Metlin, A., Paulin, L., Suomalainen, S., Neuvonen, E., Rybakov, S., Mikhalishin, V., Huovilainen, A., 2008. Characterization of Russian rabies virus vaccine strain RV-97. Virus Res. 132, 242–247.
Mifune, K., Makino, Y., Mannen, K., 1979. Susceptibility of various cell lines to rabies virus. Japan. J. Trop. Med. Hyg. 7, 201–208.
Minamoto, N., Tanaka, H., Hishida, M., Goto, H., Ito, H., Naruse, S., Yamamoto, K., Sugiyama, M., Kinjo, T., Mannen, K., et al., 1994. Linear and conformation-dependent antigenic sites on the nucleoprotein of rabies virus. Microbiol. Immunol. 38, 449–455.
Ming, P., Du, J., Tang, Q., Yan, J., Nadin-Davis, S.A., Li, H., Tao, X., Huang, Y., Hu, R., Liang, G., 2009. Molecular characterization of the complete genome of a street rabies virus isolated in China. Virus Res. 143, 6–14.
Mochizuki, N., Kobayashi, Y., Sato, G., Itou, T., Gomes, A.A., Ito, F.H., Sakai, T., 2009. Complete genome analysis of a rabies virus isolate from Brazilian wild fox. Arch. Virol. 154, 1475–1488.
Morimoto, K., Foley, H.D., McGettigan, J.P., Schnell, M.J., Dietzschold, B., 2000. Reinvestigation of the role of the rabies virus glycoprotein in viral pathogenesis using a reverse genetics approach. J. Neurovirol. 6, 373–381.
Morimoto, K., Hooper, D.C., Spitsin, S., Koprowski, H., Dietzschold, B., 1999. Pathogenicity of different rabies virus variants inversely correlates with apoptosis and rabies virus glycoprotein expression in infected primary neuron cultures. J. Virol. 73, 510–518.
Morimoto, K., Kawai, A., Mifune, K., 1992. Comparison of rabies virus G proteins produced by cDNA-transfected animal cells that display either inducible or constitutive expression of the gene. J. Gen. Virol. 73, 335–345.
Morimoto, K., Ohkubo, A., Kawai, A., 1989. Structure and transcription of the glycoprotein gene of attenuated HEP-Flury strain of rabies virus. Virology 173, 465–477.
Murphy, F.A., Harrison, A.K., Winn, W.C., Bauer, S.P., 1973. Comparative pathogenesis of rabies and rabies-like viruses: infection of the central nervous system and centrifugal spread of virus to peripheral tissues. Lab. Invest. 29, 1–16.
Nagaraja, T., Madhusudana, S., Desai, A., 2008. Molecular characterization of the full-length genome of a rabies virus isolate from India. Virus Genes 36, 449–459.
Prehaud, C., Coulon, P., LaFay, F., Thiers, C., Flamand, A., 1988. Antigenic site II of the rabies virus glycoprotein: structure and role in viral virulence. J. Virol. 62, 1–7.
Pulmanausahakul, R., Li, J., Schnell, M.J., Dietzschold, B., 2008. The glycoprotein and the matrix protein of rabies virus affect pathogenicity by regulating viral replication and facilitating cell-to-cell spread. J. Virol. 82, 2330–2338.
Rasalingam, P., Rossiter, J.P., Mebatsion, T., Jackson, A.C., 2005. Comparative pathogenesis of the SAD-L16 strain of rabies virus and a mutant modifying the dynein light chain binding site of the rabies virus phosphoprotein in young mice. Virus Res. 111, 55–60.
Raux, H., Flamand, A., Blondel, D., 2000. Interaction of the rabies virus P protein with the LC8 dynein light chain. J. Virol. 74, 10212–10216.
Reed, L.J., Müench, H., 1938. A simple method of estimating fifty percent endpoints. Am. J. Hyg. 27, 493–497.
Rieder, M., Brzozka, K., Pfaller, C.K., Cox, J.H., Stitz, L., Conzelmann, K.K., 2011. Genetic dissection of interferon-antagonistic functions of rabies virus phosphoprotein: inhibition of interferon regulatory factor 3 activation is important for pathogenicity. J. Virol. 85, 842–852.
Roy, A., Hooper, D.C., 2007. Lethal silver-haired bat rabies virus infection can be prevented by opening the blood–brain barrier. J. Virol. 81, 7993–7998.
Roy, A., Hooper, D.C., 2008. Immune evasion by rabies viruses through the maintenance of blood–brain barrier integrity. J. Neurovirol. 14, 401–411.
Roy, A., Phares, T.W., Koprowski, H., Hooper, D.C., 2007. Failure to open the blood–brain barrier and deliver immune effectors to central nervous system tissues leads to the lethal outcome of silver-haired bat rabies virus infection. J. Virol. 81, 1110–1118.
Ruddock, L.W., Molinari, M., 2006. N-glycan processing in ER quality control. J. Cell Sci. 119, 4373–4380.
Saeed, M., Suzuki, R., Watanabe, N., Masaki, T., Tomonaga, M., Muhammad, A., Kato, T., Matsuura, Y., Watanabe, H., Wakita, T., Suzuki, T., 2011. Role of the endoplasmic reticulum-associated degradation (ERAD) pathway in degradation of hepatitis C virus envelope proteins and production of virus particles. J. Biol. Chem. 286, 37264–37273.
Seif, I., Coulon, P., Rollin, P.E., Flamand, A., 1985. Rabies virulence: effect on pathogenicity and sequence characterization of rabies virus mutations affecting antigenic site III of the glycoprotein. J. Virol. 53, 926–934.
Shakin-Eshleman, S.H., Remaley, A.T., Eshleman, J.R., Wunner, W.H., Spitalnik, S.L., 1992. N-linked glycosylation of rabies virus glycoprotein. Individual sequons differ in their glycosylation efficiencies and influence on cell surface expression. J. Biol. Chem. 267, 10690–10698.
Shiota, S., Mannen, K., Matsumoto, T., Yamada, K., Yasui, T., Takayama, K., Kobayashi, Y., Khawplod, P., Gotoh, K., Ahmed, K., Iha, H., Nishizono, A., 2009. Development and evaluation of a rapid neutralizing antibody test for rabies. J. Virol. Methods 161, 58–62.
Shirato, K., Miyoshi, H., Goto, A., Ako, Y., Ueki, T., Kariwa, H., Takashima, I., 2004. Viral envelope protein glycosylation is a molecular determinant of the neuroinvasiveness of the New York strain of West Nile virus. J. Gen. Virol. 85, 3637–3645.
Shoji, Y., Inoue, S., Nakamichi, K., Kurane, I., Sakai, T., Morimoto, K., 2004. Generation and characterization of P gene-deficient rabies virus. Virology 318, 295–305.
Smith, J.S., Yager, P.A., Baer, G.M., 1973. A rapid reproducible test for determining rabies neutralizing antibody. Bull. World Health Organ. 48, 535–541.
Szanto, A.G., Nadin-Davis, S.A., White, B.N., 2008. Complete genome sequence of a raccoon rabies virus isolate. Virus Res. 136, 130–139.
Takayama-Ito, M., Inoue, K., Shoji, Y., Inoue, S., Iijima, T., Sakai, T., Kurane, I., Morimoto, K., 2006a. A highly attenuated rabies virus HEP-Flury strain reverts to virulent by single amino acid substitution to arginine at position 333 in glycoprotein. Virus Res. 119, 208–215.
Takayama-Ito, M., Ito, N., Yamada, K., Minamoto, N., Sugiyama, M., 2004. Region at amino acids 164 to 303 of the rabies virus glycoprotein plays an important role in pathogenicity for adult mice. J. Neurovirol. 10, 131–135.
Takayama-Ito, M., Ito, N., Yamada, K., Sugiyama, M., Minamoto, N., 2006b. Multiple amino acids in the glycoprotein of rabies virus are responsible for pathogenicity in adult mice. Virus Res. 115, 169–175.
Tordo, N., Poch, O., Ermine, A., Keith, G., Rougeon, F., 1986. Walking along the rabies genome: is the large G-L intergenic region a remnant gene. Proc. Natl. Acad. Sci. U. S. A. 83, 3914–3918.
Tuffereau, C., Leblois, H., Benejean, J., Coulon, P., Lafay, F., Flamand, A., 1989. Arginine or lysine in position 333 of ERA and CVS glycoprotein is necessary for rabies virulence in adult mice. Virology 172, 206–212.
Vidy, A., Chelbi-Alix, M., Blondel, D., 2005. Rabies virus P protein interacts with STAT1 and inhibits interferon signal transduction pathways. J. Virol. 79, 14411–14420.

Wang, Z.W., Sarmento, L., Wang, Y., Li, X.Q., Dhingra, V., Tseggai, T., Jiang, B., Fu, Z.F., 2005. Attenuated rabies virus activates, while pathogenic rabies virus evades, the host innate immune responses in the central nervous system. J. Virol. 79, 12554–12565.

World Health Organ, 2005. WHO Expert Consultation on Rabies. World Health Organ. Tech. Rep. Ser. 931, pp. 1–88, back cover.

Wright, E., Temperton, N.J., Marston, D.A., McElhinney, L.M., Fooks, A.R., Weiss, R.A., 2008. Investigating antibody neutralization of lyssaviruses using lentiviral pseudotypes: a cross-species comparison. J. Gen. Virol. 89, 2204–2213.

Wunner, W.H., 2007. Rabies virus. In: Jackson, A.C., Wunner, W.H. (Eds.), Rabies. , 2nd ed. Academic Press, San Diego, pp. 23–68.

Veterinary Microbiology 161 (2012) 130–136

Contents lists available at SciVerse ScienceDirect

Veterinary Microbiology

journal homepage: www.elsevier.com/locate/vetmic

Isolation and phylogenetic analysis of *Bartonella* species from wild carnivores of the suborder Caniformia in Japan

Shingo Sato [a], Hidenori Kabeya [a], Tatsuya Miura [a], Kazuo Suzuki [b], Ying Bai [c], Michael Kosoy [c], Hiroshi Sentsui [d], Hiroaki Kariwa [e], Soichi Maruyama [a,*]

[a] *Laboratory of Veterinary Public Health, Department of Veterinary Medicine, College of Bioresource Sciences, Nihon University, 1866 Kameino, Fujisawa, Kanagawa 252-0880, Japan*
[b] *Hikiiwa Park Center, Tanabe, Wakayama 646-0051, Japan*
[c] *Division of Vector-Borne Diseases, Centers for Disease Control and Prevention, Fort Collins, CO 80521, USA*
[d] *Laboratory of Veterinary Epizootiology, Department of Veterinary Medicine, College of Bioresource Sciences, Nihon University, 1866 Kameino, Fujisawa, Kanagawa 252-0880, Japan*
[e] *Laboratory of Public Health, Graduate School of Veterinary Medicine, Hokkaido University, Sapporo, Hokkaido 060-0818, Japan*

ARTICLE INFO

Article history:
Received 30 March 2012
Received in revised form 6 July 2012
Accepted 10 July 2012

Keywords:
Bartonella
Caniformia
Japanese badger
Japanese marten
Wild carnivores

ABSTRACT

The prevalence of *Bartonella* species was investigated among wild carnivores of the suborder Caniformia, including 15 Japanese badgers (*Meles anakuma*), 8 Japanese martens (*Martes melampus*), 2 Japanese weasels (*Mustela itatsi*), 1 Siberian weasel (*Mustela sibirica*), 171 raccoon dogs (*Nyctereutes procyonoides*), and 977 raccoons (*Procyon lotor*) in Japan. *Bartonella* bacteria were isolated from one Japanese badger (6.7%) and from one Japanese marten (12.5%); however, no *Bartonella* species was found in other representatives of Caniformia. Phylogenetic analysis was based on concatenated sequences of six housekeeping genes (16S rRNA, *ftsZ*, *gltA*, *groEL*, *ribC*, and *rpoB*) and sequence of the 16S–23S internal transcribed spacer region. The sequence analysis indicated that the isolate derived from the Japanese badger (strain JB-15) can represent a novel *Bartonella* species and the isolate from the Japanese marten (strain JM-1) was closely related to *Bartonella washoensis*. This is the first report on isolation of *Bartonella* from badger and marten.

1. Introduction

Bartonella species are gram-negative bacteria that infect erythrocytes of various mammals (Chomel et al., 2009). Of the 24 species and three subspecies of *Bartonella* currently identified, at least twelve species are known to be zoonotic agents (Chomel et al., 2006; Raoult et al., 2006).

The order Carnivora consists of two suborders, namely Caniformia and Feliformia. In Japan, the Japanese badger (*Meles anakuma*), Japanese marten (*Martes melampus*), Japanese weasel (*Mustela itatsi*), raccoon dog (*Nyctereutes procyonoides*), and Siberian weasel (*Mustela sibirica*) are known to be native species of the suborder Caniformia. In contrast, the raccoon (*Procyon lotor*) was imported to Japan from North and Central Americas as a pet, but later the feral populations have been notably spread throughout Japan (Asano et al., 2003).

In wild carnivores in the USA, the high prevalence of *B. rochalimae* which is known to cause fever, rash, and splenomegaly in humans (Eremeeva et al., 2007) have been documented in 43% of gray foxes (*Urocyon cinereoargenteus*) and 26% of raccoons, respectively (Henn et al., 2007, 2009). The high prevalence of *B. vinsonii* subsp. *berkhoffii*, which causes endocarditis in humans was also reported in 28% of coyotes (*Canis latrans*) captured in the USA (Chang et al., 2000).

Bartonella washoensis is a causative agent of myocarditis and meningitis in humans (Kosoy et al., 2003; Probert

* Corresponding author. Tel.: +81 466 84 3636; fax: +81 466 84 3636.
E-mail address: maruyama.soichi@nihon-u.ac.jp (S. Maruyama).

0378-1135/$ – see front matter © 2012 Elsevier B.V. All rights reserved.
http://dx.doi.org/10.1016/j.vetmic.2012.07.012

et al., 2009) and the natural reservoir is considered to be the ground squirrel (*Spermophilus beecheyi*) in North America (Kosoy et al., 2003). The organism was also isolated from endocarditis in a dog in California (Chomel et al., 2003), but not from any wild carnivores in other countries.

The present study was conducted to investigate the prevalence of *Bartonella* bacteria in wild carnivores in Japan and to characterize the isolates by molecular techniques.

2. Material and methods

2.1. Sample collection

During the four-year period 2008–2011, blood samples were collected from 15 Japanese badgers, 8 Japanese martens, 3 Japanese weasels, 1 Siberian weasel, and 171 raccoon dogs in Wakayama Prefecture located in the western part of Japan. Additionally, blood samples were also collected from feral raccoons in Hokkaido ($n = 95$), Chiba ($n = 186$), and Wakayama ($n = 696$) Prefectures. All blood samples of the animals, except the raccoons, were collected from hunted, road-killed, or debilitated individuals in the field. Raccoons were captured by live cage traps and then euthanized following the guidelines for invasive alien species prepared by the Japanese Veterinary Medical Association. The blood samples were collected in EDTA-containing 2 ml blood collection tubes and then sent to the Laboratory of Veterinary Public Health at the Department of Veterinary Medicine, College of Bioresource Sciences, Nihon University. Blood samples were stored at −70 °C until examined.

2.2. Isolation of Bartonella bacteria

Frozen blood samples were thawed at room temperature and 200 μl blood aliquots were placed in sterile 1.5 ml conical tubes. The tubes were centrifuged at 1800 × *g* for 70 min; the supernatant was removed from each tube, and the sediment was mixed with 100 μl of medium 199 supplemented with 1 mM sodium pyruvate solution and 20% volume of fetal bovine serum (Life Technologies, Carlsbad, USA), and 100 μl aliquots of the mixture were plated on heart infusion agar plates (Difco, Sparks Glencoe, MI, USA) containing 5% rabbit blood (Maruyama et al., 2000). The inoculated plates were incubated at 35 °C in a moist atmosphere under 5% CO_2 for up to 4 weeks. Bacterial colonies were tentatively identified as *Bartonella* species based on colony morphology (small, gray or cream-yellow, round colonies), Gram negative staining, and the long culture period (>1 week). Five colonies were picked from each sample and each colony was subcultured using the same conditions as the primary culture.

2.3. PCR amplification and DNA sequence analysis of six housekeeping genes and ITS

The genomic DNA was extracted from each isolate by using InstaGene Matrix (Bio-Rad, Hercules, CA, USA) and submitted for identification as *Bartonella* by genus-specific PCR targeting the *gltA* gene (Inoue et al., 2008). The organisms identified as *Bartonella* were subjected to DNA sequencing of other five housekeeping genes (16S rRNA, *ftsZ*, *groEL*, *ribC*, and *rpoB*), as described previously (Inoue et al., 2011). Eight strains of *B. washoensis* (Sb944nv, AM2-1, AR2-2, CJ22-1, DR1-1, ER14-3, RJ21-1, and SR22-1) derived from squirrels were added to the phylogenetic analysis based on concatenated sequences of six housekeeping genes because of the considerable genetic variation between these strains (Inoue et al., 2011). We also applied the analysis of the 16S–23S internal transcribed spacer region (ITS) for further genetic characterization of the isolates (Houpikian and Raoult, 2001). The PCR products were purified by using the Spin Column PCR product purification kit (Bio Basic, Markham, Ontario, Canada), and then sequenced directly using the Genetic Analyzer model 3130 (Applied Biosystems, Foster City, CA, USA). A band of expected size of ITS was obtained from gel and purified by using the Wizard SV Gel and PCR Clean-Up System (Promega, Madison, WI, USA) and sub-cloned with the plasmid pGEM-T Easy vector system (Promega, Madison, WI, USA). The sequence reactions were performed by using the BigDye Terminator Cycle Sequencing Ready Reaction kit and analyzed by the same procedure as for six housekeeping genes and ITS. The sequence alignments obtained were compared with genomic sequences of prokaryotes registered in the GenBank/EMBL/DDBJ database using the BLAST program to confirm *Bartonella* species.

2.4. Phylogenetic analysis

The DNA sequences of the isolates were imported into the Lasergene sequence analysis software (DNASTAR, Madison, WI, USA) to obtain consensus sequences, and then aligned with those of type strains of known *Bartonella* species by using the CLUSTAL W program (Thompson et al., 1994). Neighbor-joining trees were constructed based on analysis of concatenated sequences for six genes (16S rRNA, *ftsZ*, *gltA*, *groEL*, *ribC*, and *rpoB*) with the Jukes–Cantor parameters method and the sequence of ITS with Kimura's 2-parameter distance method in MEGA 4.0.2 (Jukes and Cantor, 1969; Kimura, 1980; Tamura et al., 2007). Support for nodes in the trees was assessed by bootstrapping with 1000 replicates.

The sequence homologies of *gltA* and ITS between the isolates and the closest species were calculated by using GENETYX-win software, version 9 (Genetyx Corp., Tokyo, Japan).

Table 1
GenBank accession numbers for six genes and one internal spacer region of *Bartonella* isolates from Japanese badger (JB-15) and marten (JM-1).

Registered genes or region	Accession numbers for	
	JB-15	JM-1
16S rRNA	AB673447	AB611850
ftsZ	AB674230	AB611851
gltA	AB674231	AB611852
groEL	AB674232	AB611853
ribC	AB674233	AB611854
rpoB	AB674234	AB611855
ITS	AB674235	AB674236

3. Results

Bartonella bacteria were isolated from blood of one of the 15 Japanese badgers (6.7%) and one of the eight martens (12.5%). No isolates were obtained from tested Japanese weasels, raccoon dogs, Siberian weasel, or raccoons.

Strains JB-15 and JM-1, from the badger and the marten, respectively, were used as representatives for further investigation because five subcultures derived from both

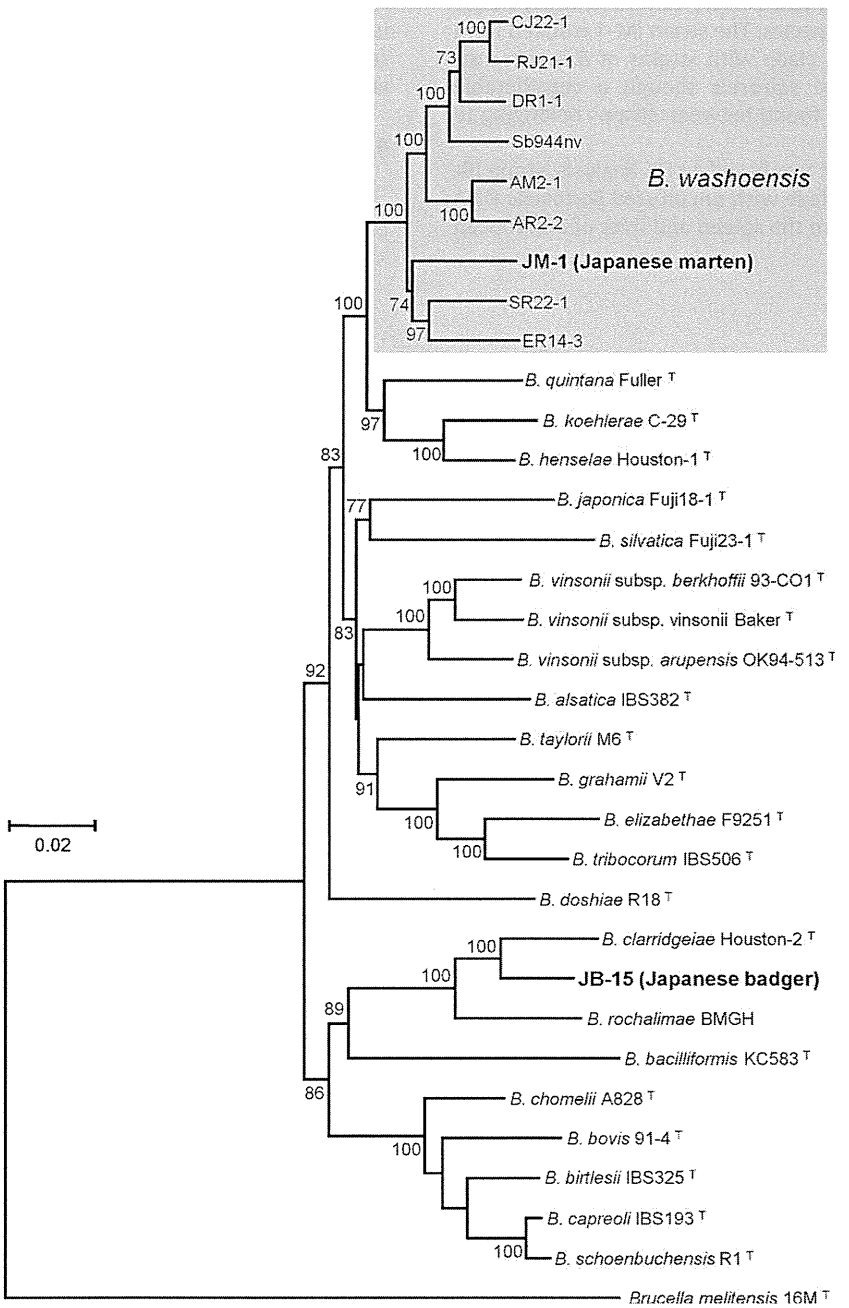

Fig. 1. Phylogenetic tree of *Bartonella* isolates (JB-15 and JM-1) and type strains of known *Bartonella* based on the concatenated sequences of six housekeeping genes (16S rRNA, *ftsZ*, *gltA*, *groEL*, *ribC*, and *rpoB*). The tree was constructed by using the neighbor-joining method with the Jukes–Cantor parameters model. Strain JB-15, JM-1, *B. rochalimae* (strain BMGH), *B. washoensis* (strains Sb944nv, AM2-1, AR2-2, CJ22-1, DR1-1, ER14-3, RJ21-1, and SR22-1) and the type strains of 21 *Bartonella* species including 3 subspecies, namely, *B. alsatica* IBS382^T, *B. bacilliformis* KC583^T, *B. bovis* 91-4^T, *B. birtlesii* IBS325^T, *B. capreoli* IBS193^T, *B. chomelii* A828^T, *B. clarridgeiae* Houston-2^T, *B. doshiae* R18^T, *B. elizabethae* F9251^T, *B. grahamii* V2^T, *B. henselae* Houston-1^T, *B. japonica* Fuji 18-1^T, *B. koehlerae* C-29^T, *B. quintana* Fuller^T, *B. schoenbuchensis* R1^T, *B. silvatica* Fuji 23-1^T, *B. taylorii* M6^T, *B. tribocorum* IBS506^T, *B. vinsonii* subsp. *arupensis* OK94-513^T, *B. vinsonii* subsp. *berkhoffii* 93-CO1^T and *B. vinsonii* subsp. *vinsonii* Baker^T were included in the phylogenetic analysis. The tree was rooted by use of *Brucella melitensis* strain 16M ^{T} as an out-group. Bootstrap values (percentages of 1000 replicates) with over 70% confidence are indicated at the tree nodes. The bar indicates 0.02 estimated nucleotide substitutions per site.

animals were genetically identical for each of the six genes. All the DNA sequences were submitted to the GenBank and accession numbers are provided in the Table 1.

A phylogenetic analysis based on the concatenated sequences of six genes suggested that the strain JB-15 isolated from the badger is distinct from all known *Bartonella* species and more likely can be described later as a novel *Bartonella* species. The strain JM-1 isolated from the marten formed a clade with strains of *B. washoensis* isolated from diverse squirrels though a considerable genetic variation was found between strains belonging to this cluster (Fig. 1).

In the phylogenetic tree based on ITS analysis, strain JB-15 formed a unique clade with uncultured *Bartonella* DNA clone T8 detected from the spleen and liver of a European badger (Fig. 2). BLAST searching has also indicated that the sequence of *gltA* from strain JB-15 was identical to that from the DNA clone 01011510020 from a European badger (Gerrikagoitia et al., 2011). The ITS sequence of strain JB-15 showed 96.7% similarity with uncultured *Bartonella* DNA clone T8 (Table 2).

Strain JM-1 formed a clade with *B. washoensis* strains isolated from squirrels based on ITS analysis (Fig. 3). The *gltA* sequence similarity between strain JM-1 and reported strains of *B. washoensis* ranged from 93.2% to 97.7% (Table 3).

4. Discussion

This is the first isolation of *Bartonella* bacteria from the badger and marten, and first detection from Asia. The

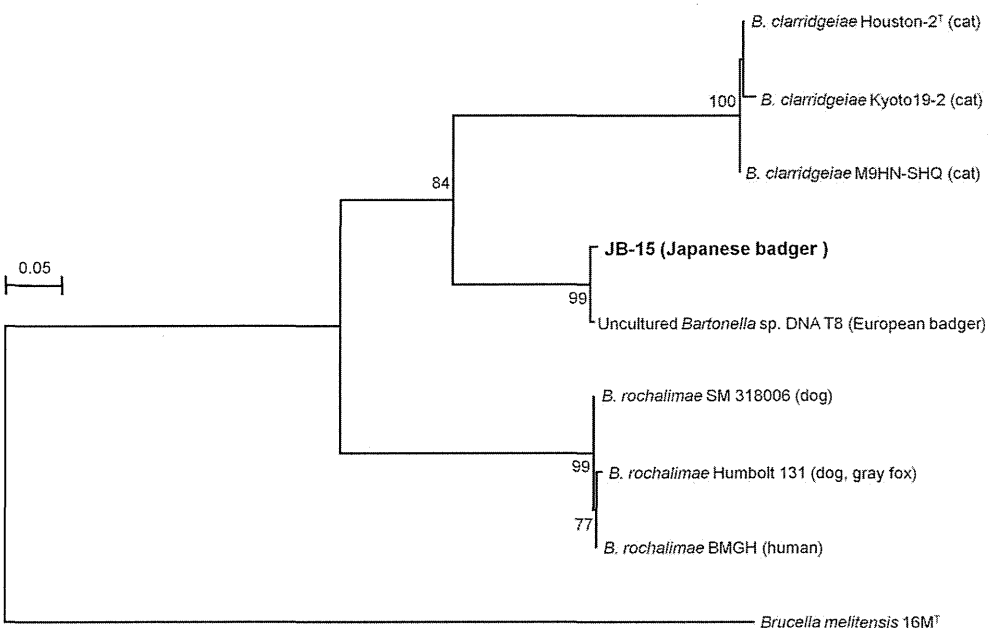

Fig. 2. Phylogenetic tree of *Bartonella* isolate (JB-15) and its related *Bartonella* strains based on the DNA sequence of ITS. The tree was constructed by using the neighbor-joining method with Kimura's 2-parameters model. Strain JB-15, *B. clarridgeiae* strains and *B. rochalimae* strains are included in the tree. Host animals of the *Bartonella* strains are shown in parentheses. The tree was rooted by using *Brucella melitensis* strain 16M ^{T} as an out-group. Bootstrap values (percentages of 1000 replicates) with over 70% confidence are indicated at the tree nodes. The bar indicates 0.05 estimated nucleotide substitutions per site.

Table 2
Sequence similarities between strain JB-15 and some closest strains of *Bartonella* in the *gltA* and ITS.

Strain	Host	% of sequence similarities to JB-15/GenBank accession number	
		gltA (312 bp)	ITS (437 bp)
Uncultured *Bartonella* sp.			
01011510020	European badger	100/GU570947	NA
T8	European badger	NA	96.7/EU098132
B. clarridgeiae			
Houston-2	Cat	96.5/U84386	65.6/AF312497
Kyoto19-2	Cat	96.5/AB674237	65.2/AB674239
M9HN-SHQ	Cat	96.3/EU770616	68.6/EU589237
B. rochalimae			
BMGH	Human	96.5/DQ683195	60.7/DQ683199
Humboldt 131	Dog, Gray fox	96.3*/DQ676484	61.3/DQ676487
SM 318006	Dog	95.9*/DQ676488	60.5/DQ676491

NA, the sequence was not available in GenBank.
* The sequence length compared was 270 bp.

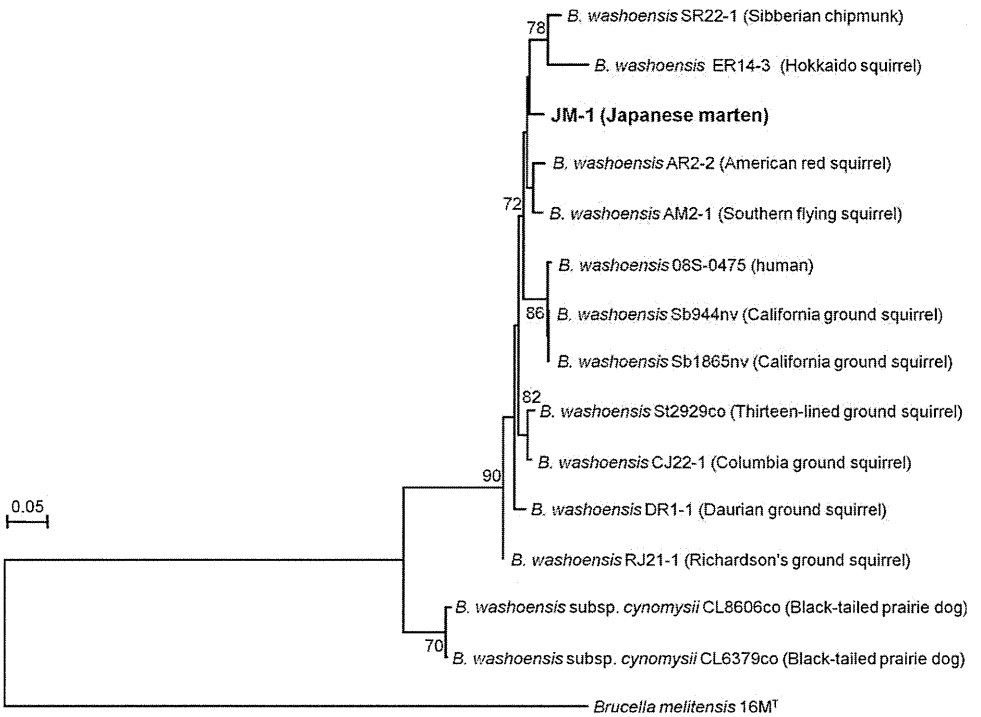

Fig. 3. Phylogenetic tree of *Bartonella* isolate (JM-1) and its related *Bartonella* strains based on the DNA sequence of ITS. The tree based on the DNA sequence of ITS was constructed by using neighbor-joining method with Kimura's 2-parameters model. Strain JM-1 and *B. washoensis* strains are included in the tree. Host animals of the *Bartonella* strains are shown in parentheses. The tree was rooted by use of *Brucella melitensis* strain 16M ^{T} as an out-group. Bootstrap values (percentages of 1000 replicates) with over 70% confidence are indicated at the tree nodes. The bar indicates 0.05 estimated nucleotide substitutions per site.

Table 3
Sequence similarities between strain JM-1 and some closest strains of *Bartonella* in the *gltA* and ITS.

Strain	Host	% of sequence similarities to JM-1/GenBank accession number	
		gltA (312 bp)	ITS (449 bp)
B. washoensis			
AR2-2	American red squirrel	95.5/AB519076	89.0/AB674246
AM2-1	Southern flying squirrel	96.8/AB444972	90.7/AB674247
CJ22-1	Columbia ground squirrel	97.4/AB444956	93.4/AB674248
DR1-1	Daurian ground squirrel	97.1/AB444962	91.5/AB674249
ER14-3	Hokkaido squirrel	93.2/AB444974	86.9/AB674250
RJ21-1	Richardson's ground squirrel	96.5/AB444959	92.6/AB674251
SR22-1	Sibberian chipmunk	97.4/AB444968	93.6/AB674252
Sb944nv	California ground squirrel	97.1/AF470616	88.2/AB674253
Sb1865nv	California ground squirrel	95.8/AB674240	88.2/AB674254
St2929co	Thirteen-lined ground squirrel	97.7*/AB674241	91.5/AB674255
08S-0875	Human	97.1/FJ719016	87.1/AB674256
B. washoensis subsp. *cynomysii*			
CL8606co	Black-tailed prairie dog	96.7/DQ897367	88.4†/AB674257
CL6379co	Black-tailed prairie dog	96.5/AY589564	95.2†/AB674258

* The sequence length compared is 306 bp.
† The sequence length compared is 293 bp.

phylogenetic analysis based on the concatenated sequences of six housekeeping genes showed that the strain JB-15 from the Japanese badger appears to be different from other known *Bartonella* species. On the other hand, strain JM-1 from the Japanese marten is relatively close to *B. washoensis*. In our previous study, the considerable genetic variation has been found among the isolates of squirrels (Inoue et al., 2011). In the present study, strain JM-1 formed a large clade with *B. washoensis* strains, suggesting that the strain may belong to *B. washoensis*.

Phylogenetic analysis of ITS is recognized to be an useful tool to identify *Bartonella* species (Houpikian and Raoult, 2001). Therefore, in addition to six housekeeping

genes, we utilized the ITS region for further genetic characterization of the *Bartonella* species isolated from wild Caniformia in Japan. Strain JB-15 was distinct from other known *Bartonella* species according to the phylogenetic analysis of ITS. It was also found that the sequence of ITS from strain JB-15 was closest (96.7%) to that of uncultured *Bartonella* DNA from a European badger (*Meles meles*) captured in northern Spain (Gerrikagoitia et al., 2011). The sequence of *gltA* from strain JB-15 was identical to the DNA detected in the European badger. The Japanese badger is taxonomically related to the European badger (Kurose et al., 2001). Interestingly, badgers in both Asia and Europe were infected with similar *Bartonella* species. More samples are needed to investigate whether badgers in other countries harbor similar *Bartonella* species.

The analysis based on *gltA* supported the similarity between strain JM-1 and previously reported strains of *B. washoensis* (AM2-1, CJ22-1, DR1-1, RJ21-1, SR22-1, Sb944nv, St2929co, 08S-0875, CL8606co, and CL6379co); the sequence identity was above the cut-off value (>96.0%) accepted for differentiation of *Bartonella* species (La Scola et al., 2003). In addition, the sequence of ITS from strain JM-1 also demonstrated the closeness to *B. washoensis* strains obtained from squirrels and the strain formed a clade with *B. washoensis* strains in the phylogenetic analysis of ITS. Generally, *Bartonella* species are recognized as host-specific parasitic bacteria; however, evidence that the *Bartonella* species could occasionally jump from the natural reservoir to other mammals has been documented (Bai et al., 2007). Since only one of the eight martens was found to be bacteremic in the present study, more samples are necessary to show the possibility that martens are the natural reservoir or accidental host of *B. washoensis*.

Although raccoons in the USA frequently harbor *B. rochalimae* (11/42; 26.2%), no *Bartonella* was isolated from feral raccoons in Japan despite testing 977 samples. It has been reported that *Pulex* fleas carrying DNA of *B. vinsonii* subsp. *berkhoffii* and *B. rochalimae* infest wild carnivores, suggesting that the fleas could be a potential vector for transmission of *Bartonella* agents among wild carnivores in the USA (Gabriel et al., 2009). We have no information about infestation of Japanese carnivores with *Pulex*. Another possible explanation for the absence of *Bartonella* in raccoons can be a historical situation when non-bacteremic animals were originally introduced to Japan.

No *Bartonella* was isolated from Japanese weasels or Siberian weasel, but the sample size was small for making any conclusion. Although *Bartonella* were not isolated from raccoon dogs, *Bartonella* DNA was detected in 11 of 171 animals (6.4%) by PCR amplification of *gltA* and *rpoB* genes and all of the amplicons were found to be closest to *B. rochalimae* by the sequence analysis of both genes (data not shown). It is possible that culturing of *Bartonella* from raccoon dogs require different culturing conditions. For example, we know that temperature at 28 °C without CO_2 is recommended for culturing *B. bacilliformis* (Ellis et al., 1999).

More than 70% of emerging infections have been thought to come from wildlife (Kuiken et al., 2005). Increased outdoor activities might result in higher risk of exposure to various types of zoonoses (Boulouis et al., 2005; Breitschwerdt et al., 2007). Previous studies have shown that wild carnivores may play an important role as potential reservoirs for zoonotic *Bartonella* (Breitschwerdt et al., 2005; Henn et al., 2007). Comprehensive surveillance should be done to determine a prevalence and distribution of *Bartonella* species in wildlife in Japan and to clarify their role as potential human pathogens.

Acknowledgements

This work was supported in part by a Grant-in-Aid for Scientific Research (no. 23580429), and Strategic Research Base Development Program, International Research on Epidemiology of Zoonoses and Training for Young Researchers by Ministry of Education, Culture, Sports, Science and Technology, Japan. It was also supported in part by a Grant-in-Aid from Ministry of Health, Labour and Welfare, Japan.

References

Asano, M., Matoba, Y., Ikeda, T., Suzuki, M., Asakawa, M., Ohtaishi, N., 2003. Reproductive characteristics of the feral raccoon (*Procyon lotor*) in Hokkaido, Japan. J. Vet. Med. Sci. 65, 369–373.

Bai, Y., Kosoy, M.Y., Cully, J.F., Bala, T., Ray, C., Collinge, S.K., 2007. Acquisition of nonspecific *Bartonella* strains by the northern grasshopper mouse (*Onychomys leucogaster*). FEMS Microbiol. Ecol. 61, 438–448.

Boulouis, H.J., Chang, C.C., Henn, J.B., Kasten, R.W., Chomel, B.B., 2005. Factors associated with the rapid emergence of zoonotic *Bartonella* infections. Vet. Res. 36, 383–410.

Breitschwerdt, E.B., Hegarty, B.C., Maggi, R., Hawkins, E., Dyer, P., 2005. *Bartonella* species as a potential cause of epistaxis in dogs. J. Clin. Microbiol. 43, 2529–2533.

Breitschwerdt, E.B., Maggi, R.G., Duncan, A.W., Nicholson, W.L., Hegarty, B.C., Woods, C.W., 2007. *Bartonella* species in blood of immunocompetent persons with animal and arthropod contact. Emerg. Infect. Dis. 13, 938–941.

Chang, C.C., Kasten, R.W., Chomel, B.B., Simpson, D.C., Hew, C.M., Kordick, D.L., Heller, R., Piemont, Y., Breitschwerdt, E.B., 2000. Coyotes (*Canis latrans*) as the reservoir for a human pathogenic *Bartonella* sp.: molecular epidemiology of *Bartonella vinsonii* subsp. *berkhoffii* infection in coyotes from central coastal California. J. Clin. Microbiol. 38, 4193–4200.

Chomel, B.B., Wey, A.C., Kasten, R.W., 2003. Isolation of *Bartonella washoensis* from a dog with mitral valve endocarditis. J. Clin. Microbiol. 41, 5327–5332.

Chomel, B.B., Boulouis, H.J., Maruyama, S., Breitschwerdt, E.B., 2006. *Bartonella* spp. in pets and effect on human health. Emerg. Infect. Dis. 12, 389–394.

Chomel, B.B., Boulouis, H.J., Breitschwerdt, E.B., Kasten, R.W., Vayssier-Taussat, M., Birtles, R.J., Koehler, J.E., Dehio, C., 2009. Ecological fitness and strategies of adaptation of *Bartonella* species to their hosts and vectors. Vet. Res. 40, 29.

Ellis, B.A., Rotz, L.D., Leake, J.A., Samalvides, F., Bernable, J., Ventura, G., Padilla, C., Villaseca, P., Beati, L., Regnery, R., Childs, J.E., Olson, J.G., Carrillo, C.P., 1999. An outbreak of acute bartonellosis (Oroya fever) in the Urubamba region of Peru, 1998. Am. J. Trop. Med. Hyg. 61, 344–349.

Eremeeva, M.E., Gerns, H.L., Lydy, S.L., Goo, J.S., Ryan, E.T., Mathew, S.S., Ferraro, M.J., Holden, J.M., Nicholson, W.L., Dasch, G.A., Koehler, J.E., 2007. Bacteremia, fever, and splenomegaly caused by a newly recognized *Bartonella* species. N. Engl. J. Med. 356, 2381–2387.

Gabriel, M.W., Henn, J., Foley, J.E., Brown, R.N., Kasten, R.W., Foley, P., Chomel, B.B., 2009. Zoonotic *Bartonella* species in fleas collected on gray foxes (*Urocyon cinereoargenteus*). Vector Borne Zoonotic Dis. 9, 597–602.

Gerrikagoitia, X., Gil, H., Garcia-Esteban, C., Anda, P., Juste, R.A., Barral, M., 2011. Presence of *Bartonella* species in wild carnivores from Northern Spain. Appl. Environ. Microbiol. 78, 885–888.

Henn, J.B., Gabriel, M.W., Kasten, R.W., Brown, R.N., Theis, J.H., Foley, J.E., Chomel, B.B., 2007. Gray foxes (*Urocyon cinereoargenteus*) as a potential reservoir of a *Bartonella clarridgeiae*-like bacterium and domestic dogs as part of a sentinel system for surveillance of zoonotic arthropod-borne pathogens in northern California. J. Clin. Microbiol. 45, 2411–2418.

Henn, J.B., Chomel, B.B., Boulouis, H.J., Kasten, R.W., Murray, W.J., Bar-Gal, G.K., King, R., Courreau, J.F., Baneth, G., 2009. *Bartonella*

rochalimae in raccoons, coyotes, and red foxes. Emerg. Infect. Dis. 15, 1984–1987.

Houpikian, P., Raoult, D., 2001. 16S/23S rRNA intergenic spacer regions for phylogenetic analysis, identification, and subtyping of *Bartonella* species. J. Clin. Microbiol. 39, 2768–2778.

Inoue, K., Maruyama, S., Kabeya, H., Yamada, N., Ohashi, N., Sato, Y., Yukawa, M., Masuzawa, T., Kawamori, F., Kadosaka, T., Takada, N., Fujita, H., Kawabata, H., 2008. Prevalence and genetic diversity of *Bartonella* species isolated from wild rodents in Japan. Appl. Environ. Microbiol. 74, 5086–5092.

Inoue, K., Kabeya, H., Hagiya, K., Kosoy, M.Y., Une, Y., Yoshikawa, Y., Maruyama, S., 2011. Multi-locus sequence analysis reveals host specific association between *Bartonella washoensis* and squirrels. Vet. Microbiol. 148, 60–65.

Jukes, T.H., Cantor, C.R., 1969. Evolution of protein molecules. In: Munro, H.N. (Ed.), Mammalian Protein Metabolism, vol. 3. Academic Press, New York, pp. 21–132.

Kimura, M., 1980. A simple method for estimating evolutionary rates of base substitutions through comparative studies of nucleotide sequences. J. Mol. Evol. 16, 111–120.

Kosoy, M., Murray, M., Gilmore Jr., R.D., Bai, Y., Gage, K.L., 2003. *Bartonella* strains from ground squirrels are identical to *Bartonella washoensis* isolated from a human patient. J. Clin. Microbiol. 41, 645–650.

Kuiken, T., Leighton, F.A., Fouchier, R.A., LeDuc, J.W., Peiris, J.S., Schudel, A., Stohr, K., Osterhaus, A.D., 2005. Public health. Pathogen surveillance in animals. Science 309, 1680–1681.

Kurose, N., Kaneko, Y., Abramov, A.V., Siriaroonrat, B., Masuda, R., 2001. Low genetic diversity in Japanese populations of the Eurasian badger *Meles meles* (Mustelidae, Carnivora) revealed by mitochondrial cytochrome b gene sequences. Zoolog. Sci. 18, 1145–1151.

La Scola, B., Zeaiter, Z., Khamis, A., Raoult, D., 2003. Gene-sequence-based criteria for species definition in bacteriology: the *Bartonella* paradigm. Trends Microbiol. 11, 318–321.

Maruyama, S., Nakamura, Y., Kabeya, H., Tanaka, S., Sakai, T., Katsube, Y., 2000. Prevalence of *Bartonella henselae*, *Bartonella clarridgeiae* and the 16S rRNA gene types of *Bartonella henselae* among pet cats in Japan. J. Vet. Med. Sci. 62, 273–279.

Probert, W., Louie, J.K., Tucker, J.R., Longoria, R., Hogue, R., Moler, S., Graves, M., Palmer, H.J., Cassady, J., Fritz, C.L., 2009. Meningitis due to a "*Bartonella washoensis*"-like human pathogen. J. Clin. Microbiol. 47, 2332–2335.

Raoult, D., Roblot, F., Rolain, J.M., Besnier, J.M., Loulergue, J., Bastides, F., Choutet, P., 2006. First isolation of *Bartonella alsatica* from a valve of a patient with endocarditis. J. Clin. Microbiol. 44, 278–279.

Tamura, K., Dudley, J., Nei, M., Kumar, S., 2007. MEGA4: molecular evolutionary genetics analysis (MEGA) software version 4.0. Mol. Biol. Evol. 24, 1596–1599.

Thompson, J.D., Higgins, D.G., Gibson, T.J., 1994. CLUSTAL W: improving the sensitivity of progressive multiple sequence alignment through sequence weighting, position-specific gap penalties and weight matrix choice. Nucleic Acids Res. 22, 4673–4674.

Comparative Immunology, Microbiology and Infectious Diseases 35 (2012) 575–581

Contents lists available at SciVerse ScienceDirect

Comparative Immunology, Microbiology and Infectious Diseases

journal homepage: www.elsevier.com/locate/cimid

Prevalence and genetic diversity of *Bartonella* species in sika deer (*Cervus nippon*) in Japan

Shingo Sato[a], Hidenori Kabeya[a], Mari Yamazaki[a], Shinako Takeno[a], Kazuo Suzuki[b], Shinichi Kobayashi[c], Kousaku Souma[d], Takayoshi Masuko[d], Bruno B. Chomel[e], Soichi Maruyama[a,*]

[a] *Laboratory of Veterinary Public Health, Department of Veterinary Medicine, College of Bioresource Sciences, Nihon University, 1866 Kameino, Fujisawa, Kanagawa 252-0880, Japan*
[b] *Hikiiwa Park Center, Tanabe, Wakayama 646-0051, Japan*
[c] *Laboratory of Management of Animal Industry, Department of Animal Science and Resources, College of Bioresource Sciences, Nihon University, 1866 Kameino, Fujisawa, Kanagawa 252-0880, Japan*
[d] *Laboratory of Animal Productive Management, Department of Bioproduction, Faculty of Bioindustry, Tokyo University of Agriculture, 196 Yasaka, Abashiri, Hokkaido 099-2493, Japan*
[e] *Department of Population Health and Reproduction, School of Veterinary Medicine, University of California, Davis, CA 95616, USA*

ARTICLE INFO

Article history:
Received 20 March 2012
Received in revised form 25 June 2012
Accepted 3 July 2012

Keywords:
Bartonella
Prevalence
Deer
Japan

ABSTRACT

We report the first description of *Bartonella* prevalence and genetic diversity in 64 Honshu sika deer (*Cervus nippon centralis*) and 18 Yezo sika deer (*Cervus nippon yesoensis*) in Japan. Overall, *Bartonella* bacteremia prevalence was 41.5% (34/82). The prevalence in wild deer parasitized with ticks and deer keds was 61.8% (34/55), whereas no isolates were detected in captive deer (0/27) free of ectoparasites. The isolates belonged to 11 genogroups based on a combination of the *gltA* and *rpoB* gene sequences. Phylogenetic analysis of concatenated sequences of the *ftsZ*, *gltA*, *ribC*, and *rpoB* genes of 11 representative isolates showed that Japanese sika deer harbor three *Bartonella* species, including *B. capreoli* and two novel *Bartonella* species. All Yezo deer's isolates were identical to *B. capreoli* B28980 strain isolated from an elk in the USA, based on the sequences of the *ftsZ*, *gltA*, and *rpoB* genes. In contrast, the isolates from Honshu deer showed a higher genetic diversity.

1. Introduction

Bartonella species are Gram-negative bacteria that infect the erythrocytes of various mammals, and are putatively transmitted by blood-feeding arthropods [1–3]. Various mammalian species, such as canines, felines, rodents, and ruminants are the reservoir hosts of *Bartonella*, and 11 of the 26 *Bartonella* species or subspecies are recognized to be zoonotic agents [4–6].

Several epidemiological studies of *Bartonella* in domestic and wild ruminants reported that roe deer (*Capreolus capreolus*) in France [7] and elk (*Cervus elaphus*) in Wyoming, USA [8], and roe deer in Germany [9] and cows in France [10] harbor *B. capreoli* and *B. schoenbuchensis*, respectively. Mule deer (*Odocoileus hemionus*) and elk in the USA have also been found to carry *Bartonella bovis* [11], which was first isolated from a cow in France [7]. Domestic cattle in France [12] and New Caledonia [13] have been shown to harbor *Bartonella chomelii*, which is thought to have been brought with cattle from France to New Caledonia. Recently, sheep were identified as natural hosts of candidatus *Bartonella melophagi* in the USA [14], which is a species pathogenic for humans [15]. *B. bovis* was reported

* Corresponding author. Tel.: +81 466 84 3636; fax: +81 466 84 3636.
E-mail address: maruyama.soichi@nihon-u.ac.jp (S. Maruyama).

0147-9571/$ – see front matter © 2012 Elsevier Ltd. All rights reserved.
http://dx.doi.org/10.1016/j.cimid.2012.07.001

to cause endocarditis in cattle [16], while the pathogenicity of other ruminant-associated *Bartonella* species except candidatus *B. melophagi* for humans and animals is still unknown.

B. schoenbuchensis was isolated from European deer keds (*Lipoptena cervi*) in Germany [3]. In addition, the DNA of *B. chomelii* and *B. schoenbuchensis* was detected from European deer keds in France [17], and the latter was also found in both European [18] and neotropical deer keds (*Lipoptena mazamae*) in the USA [19]. In contrast, viable *Bartonella* species were not found in ticks collected from ruminants though the DNA of *B. capreoli* and *B. schoenbuchensis* was detected from sheep tick (*Ixodes ricinus*) in Poland [20] and deer tick (*Ixodes scapularis*) in the USA [18], respectively. Since several *Bartonella* species were isolated from deer keds collected from wild deer, these ectoparasites have been thought to be a possible vector in deer. On the other hand, ticks are less likely to be another vector.

Recently, the population of Japanese sika deer (*Cervus nippon*) has been significantly expanding throughout Japan [21], and animals are now sharing human environment. Furthermore, wild deer are recognized to be infectious sources of zoonoses, such as hepatitis E, salmonellosis, and brucellosis [22,23]. Therefore, it is important to investigate the prevalence of *Bartonella* species in deer and determine which species are present from the standpoint of public health.

The aim of the present study was to investigate the prevalence of *Bartonella* species among wild and captive sika deer in Japan and to characterize the isolates by molecular biological techniques.

2. Materials and methods

2.1. Sample collection

During November 2008 to October 2010, blood samples (2–7 ml) were collected from 64 Honshu deer (*C. nippon centralis*) and 18 Yezo deer (*C. nippon yesoensis*) in Japan. Thirty-seven Honshu deer and 18 Yezo deer were free-ranging wild deer, and were hunted in Wakayama, Nara, and Hokkaido Prefectures. A total of 27 Honshu deer were captive and raised in rearing facilities in Aichi and Miyagi Prefectures. Most of the free-ranging wild deer were infested with deer keds (*Lipoptena fortisetosa*) and/or *Haemaphysalis* and *Ixodes* ticks, while no ectoparasites were detected on the captive deer, as most of these deer ($n = 23$) had been treated with ivermectin and four of them were raised as breeding animals.

The blood samples of wild deer were immediately collected from the heart of carcass and those of captive deer were collected from cervical vein of anesthetized individuals. All blood samples were transferred into EDTA-containing collection tubes and sent to the Laboratory of Veterinary Public Health, Department of Veterinary Medicine, College of Bioresource Sciences, Nihon University. These samples were stored at −70 °C until examined.

2.2. Isolation of bacterial strains

Frozen blood samples were thawed at room temperature, and 200 μl blood aliquots were separated into 1.5 ml conical tubes. The tubes were centrifuged at 1800 × *g* for 70 min. After centrifugation, the supernatants were removed from the tubes, and each sediment was mixed with 100 μl of medium 199 supplemented with sodium pyruvate solution and fetal bovine serum (Life Technologies, Carlsbad, CA, USA). Aliquots (100 μl) of the mixture were plated on heart infusion agar plates (Difco, Sparks Glencoe, MI, USA) containing 5% rabbit blood [7,12,24]. The inoculated plates were incubated at 35 °C in a moist atmosphere under 5% CO_2 for up to 4 weeks. Bacterial colonies were tentatively identified as *Bartonella* based on colony morphology (small, gray or cream-yellow, round colonies), and subsequently 5 colonies were picked up from each sample, and sub-cultured on a fresh blood agar plate using the same conditions as the primary culture.

2.3. PCR amplification and DNA sequencing

Genomic DNA was extracted from whole bacterial cells by using a commercial kit, Instagene matrix (Bio-Rad, Hercules, CA, USA) and subjected to genus-specific PCR targeting the citrate synthase gene (*gltA*) and RNA polymerase beta-subunit-encoding gene (*rpoB*) to identify *Bartonella*. The PCR was performed with 20 μl mixtures containing 20 ng of DNA, 200 μM of each deoxynucleoside triphosphate, 1.5 mM $MgCl_2$, 0.5 U *Taq* DNA polymerase (Promega, Madison, WI, USA), and 1 pmol of each primer. Positive and negative controls were prepared by extracting DNA from *Bartonella doshiae* R-18^T and double-distilled water, respectively. Primers used for the amplification of *gltA* [25] and *rpoB* [26] have been previously described. The products were analyzed by electrophoresis on 2% agarose gels, and the target bands were detected by staining gels with ethidium bromide and viewing under UV light.

The PCR products were purified by using the Spin Column PCR product purification kit (Bio Basic, Ontario, Canada), and then sequenced directly by using the BigDye Terminator Cycle Sequencing Ready Reaction kit and a Genetic Analyzer model 3130 (Applied Biosystems, Foster City, CA, USA) as recommended by the manufacturer's instructions. The sequence alignments obtained in this study were compared with those of other known *Bartonella* species deposited in the GenBank/EMBL/DDBJ database by using the BLAST program. The Clustal W program within GENETYX-win software, version 9 (Genetyx Corp., Tokyo, Japan) was used to compare homologous *gltA* and *rpoB* sequences to identify genetic variants. The combination of the *gltA* and *rpoB* gene sequences gave a total of 11 genogroups, and a representative isolate from each of the 11 genogroups was used for additional PCR and sequence analysis of the cell division protein gene (*ftsZ*) and the riboflavin synthase gene (*ribC*). Primers used for the amplification of *ftsZ* [27] and *ribC* [28] have been previously described. The sequences of *ftsZ*, *gltA*, *ribC*, and *rpoB* from the representative isolates have been submitted to GenBank/EMBL/DDBJ and assigned accession numbers.

Table 1
Prevalence of *Bartonella* bacteria in Japanese sika deer and the state of ectoparasite infestation.

Habitat of deer	Prefecture	Subspecies of deer	Ectoparasite infestation[a]	No. of deer examined	No. of positive deer (%)
Wild	Hokkaido	Yezo deer	+	18	9(50.0)
	Nara	Honshu deer	+	16	12(75.0)
	Wakayama	Honshu deer	+	21	13(61.9)
		Subtotal		55	34(61.8)[†]
Captive	Aichi	Honshu deer	–	23	0
	Miyagi	Honshu deer	–	4	0
		Subtotal		27	0
		Total		82	34(41.5)[†]

[a] Ectoparasites consisted of deer keds and/or *Haemaphysalis* and *Ixodes* ticks.
[†] $p < 0.001$, versus prevalence of the captive deer.

2.4. Construction of a phylogenetic tree based on ftsZ, gltA, ribC, and rpoB

A phylogenetic tree was constructed based on the concatenated sequences of *ftsZ*, *gltA*, *ribC*, and *rpoB* by using the neighbor-joining method with the Jukes–Cantor parameter method within MEGA 4.0.2 software [29,30]. Eleven representative isolates from Japanese sika deer examined, the ruminant-associated *Bartonella* species (*B. bovis* 91-4^T, *B. capreoli* IBS193^T, *B. capreoli* B28980, *B. chomelii* A828^T, *B. schoenbuchensis* R1^T, and candidatus *B. melophagi* K-2C), and other known *Bartonella* species were included in the analysis. Bootstrap analysis was performed with 1000 trials of bootstrap data (bootstrap values lower than 70% are not shown in the tree).

2.5. Statistical analysis

Statistical analysis was performed using the statistical package StatMate III for Windows, Release 2005 (ATMS, Corp., Tokyo, Japan). Chi-square tests were used to examine the statistical significance; $p < 0.05$ was considered as significant.

3. Results

3.1. Prevalence of Bartonella bacteremia

Various numbers of colonies, ranging from 20 to more than 500, appeared on the agar plates when *Bartonella* bacteria were detected. The overall prevalence of *Bartonella* bacteremia in Japanese sika deer was 41.5% (34/82). *Bartonella* bacteria were isolated from 61.8% (34/55) of the wild deer, whereas no isolates were obtained from the captive deer (0/27). Many ectoparasites such as deer keds and/or ticks were detected throughout the body of wild deer only and not in captive deer. *Bartonella* prevalence in wild deer was 50.0% (9/18) in Hokkaido, 75.0% (12/16) in Nara, and 61.9% (13/21) in Wakayama Prefectures; no significant difference was observed among the three prefectures (Table 1).

3.2. Phylogenetic analysis and genetic diversity of Bartonella isolates

Based on a phylogenetic analysis of the concatenated sequences of *ftsZ*, *gltA*, *ribC*, and *rpoB* genes, the 11 representative isolates formed three clusters designated lineages A, B, and C. Strains Honshu-8.1, Honshu-18.2, and Yezo-25.1 were grouped in lineage A with *B. capreoli* IBS193^T isolated from a roe deer in France and *B. capreoli* B28980 isolated from an elk in the USA. The strains in lineages B and C were distinct from other known *Bartonella* species (Fig. 1).

The sequences of *ftsZ*, *gltA* and *rpoB* genes from strain Yezo-25.1 were identical to those of *B. capreoli* B28980. Strains Honshu-8.1 and Honshu-18.2 in lineage A showed the highest similarities with *B. capreoli* IBS193^T or B28980 for *gltA* (99.4%) and *rpoB* (98.4–98.9%) genes. In contrast, the sequence similarities for *gltA* and *rpoB* between the strains in lineage B (Honshu-9.1, Honshu-9.3, Honshu-11.1, Honshu-12.1, Honshu-18.5, Honshu-53.5, and Honshu-58.5) and the ruminant-associated *Bartonella* species ranged from 93.6 to 94.6% and 96.5 to 97.6%, respectively. Comparing the sequences of *gltA* and *rpoB* between Honshu-16.1 and the ruminant-associated *Bartonella* species, the similarities were 93.6% and 95.3%, respectively (Table 2).

The sequence similarities for *gltA* and *rpoB* genes among seven strains in lineage B ranged from 98.1 to 100% and 97.1 to 100%, respectively. Strain Honshu-16.1 in lineage C showed the lowest similarities with the strains in lineage B for both *gltA* (93.9–94.6%) and *rpoB* (94.5–95.0%) genes (Table 3).

Honshu deer harbored three *Bartonella* species designated as lineages A (*B. capreoli*), B, and C. Lineage B was dominant (20/37; 54.1%) in Honshu deer. In addition, 8 (21.6%) of the Honshu deer were co-infected with *B. capreoli* and the strains belonging to lineage B. In contrast, Yezo deer harbored only strains belonging to lineage A (Table 4).

4. Discussion

The present study provides the first evidence of *Bartonella* species infecting 61.8% (34/55) of wild Japanese

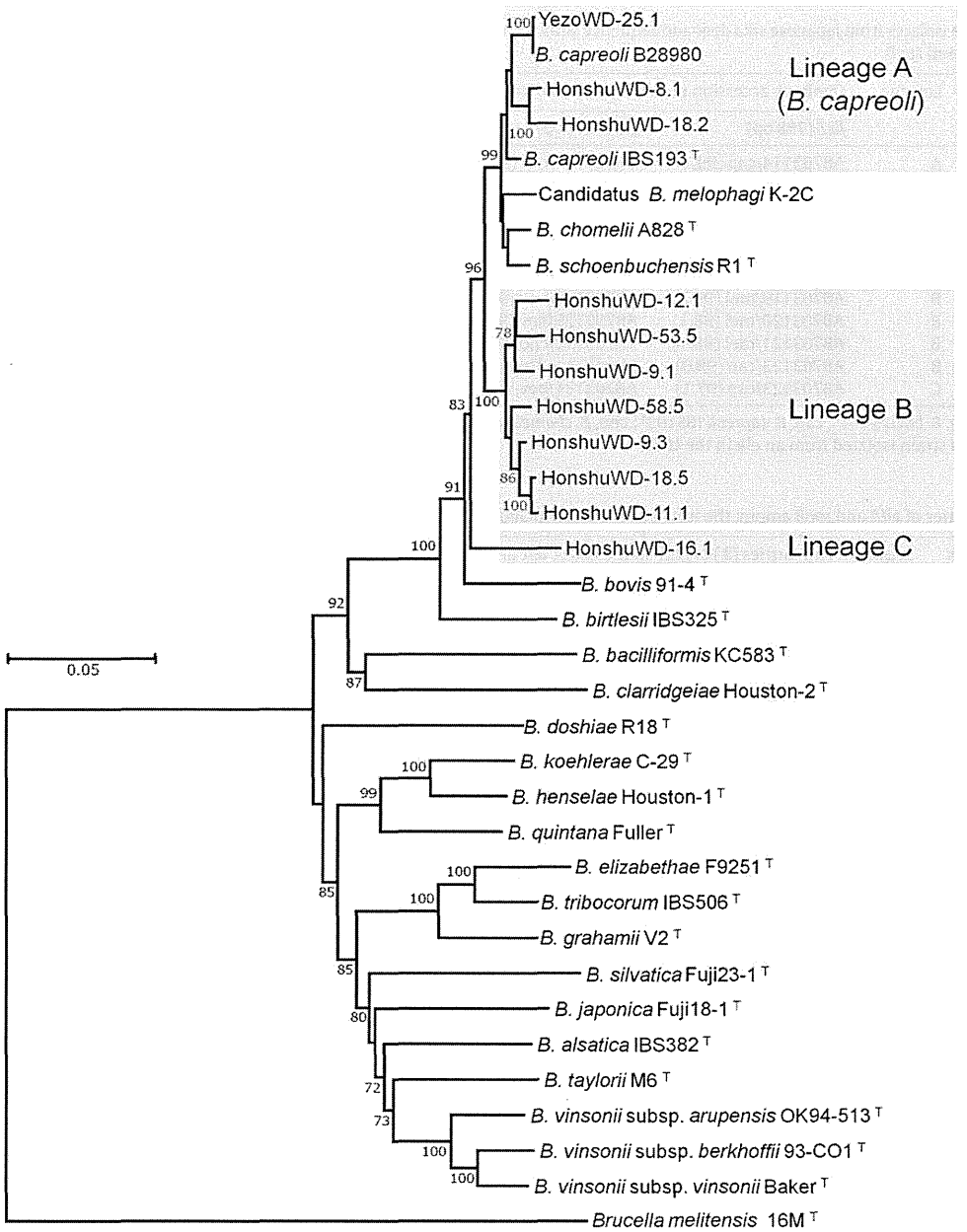

Fig. 1. Phylogenetic tree of *Bartonella* isolates from Japanese sika deer and other known *Bartonella* species based on the concatenated sequences of 4 housekeeping genes (*ftsZ*, *gltA*, *ribC*, and *rpoB*). The tree was constructed by using neighbor-joining method with Jukes–Cantor parameter model. Eleven representative *Bartonella* isolates (Honshu-8.1, -9.1, -9.3, -11.1, -12.1, -16.1, -18.2, -18.5, -53.5, -58.5, and Yezo-25.1) from Japanese sika deer, the ruminant-associated *Bartonella* species (*B. bovis* 91-4^T, *B. capreoli* IBS193^T, *B. capreoli* B28980, *B. chomelii* A828^T, *B. schoenbuchensis* R1^T, and candidatus *B. melophagi* K-2C), and other known *Bartonella* species were included in the tree. The tree is rooted by use of *Brucella melitensis* strain 16M^T as an out-group. Bootstrap values (percentages of 1000 replicates) with over 70% confidence are indicated at the tree nodes. The bar indicates 0.05 estimated nucleotide substitutions per site.

sika deer. Similarly, high prevalence of *B. bovis* and *B. schoenbuchensis* has been reported in 90% (38/42) of mule deer in CA, USA [11] and 80% (4/5) of roe deer in Germany [9]. *Bartonella capreoli* was also isolated from roe deer in France [7]. *Bartonella* DNA has also been detected in 39% (23/59) of the roe deer and 35% (7/20) of the red deer in Poland [31]. Thus, a high prevalence of *Bartonella* infection was observed in various species of deer in other countries.

In the present study, *Bartonella* bacteria were found only in wild deer, but not in captive deer. Although a number of ectoparasites including deer keds and *Haemaphysalis* and *Ixodes* ticks were found on the wild deer, no ectoparasites were detected on the captive deer, as most of the animals had been treated with ivermectin. DNA from several *Bartonella* species has been detected in both deer keds and ticks collected from wild deer in the USA [18,19] and in European